7

Organization of Interface and Matrix Containing Fillers

This chapter analyzes how a filler is distributed in materials and what interaction occurs between the filler and the matrix. These two factors make a major contribution to reinforcement of the filled materials. We will outline the principles governing filler distribution and interaction and explain the relevance of reported studies. Chapters 5, 6, and 10 contain discussion of other related phenomena such as particle size of fillers, chemical reactivity in filled systems, and morphology, respectively. Chapter 8 shows impact of organization and filler presence on mechanical properties of filled systems. The information included in the above chapters helps us to understand how to use fillers to improve the performance of a material.

7.1 PARTICLE DISTRIBUTION IN MATRIX

Idealized distribution of filler particles in a matrix can be predicted by various models as discussed in Chapter 5. Here, an attempt is made to examine empirical data on filler distribution and to determine factors in actual filler which cause that distribution differs from an ideal model used to predict packing density of the filler.

Filler particles generated *in situ* can be perceived as ideally distributed within the matrix. Experimental studies show that the situation is more complex.[1] Poly(dimethyl siloxane) network was swollen to equilibrium in tetraethyl-orthosilicate which was then hydrolyzed to produce an *in situ* filler. Such an experiment gives the almost ideal conditions of uniform distribution because both matrix and the filler precursor are chemically similar. There are numerous factors which affect how uniformly a filler is distributed. These include:

- The choice of hydrolysis catalyst
- The hydrolysis time
- The sample thickness

The most uniform distribution was obtained when the hydrolysis time was long, sample was thin, and the catalyst basic. If conditions were reversed (short hydrolysis time, bulky sample, and acidic catalyst), filler was preferentially formed on the peripheries of the sample. What is the force which drives the precursor out of its initial equilibrium? The most likely scenario is that a fast process leads to the

formation of a silica skin which inhibits the transport of the water required to hydrolyze the inside layers of the precursor. Under such circumstances, tetraethylorthosilicate, even though it is a larger molecule than water, diffuses to the surface to equilibrate its concentration to replace the already converted portions.

In another similar example nanocomposite was formed in a polyurethane matrix.[2] Solvent soluble polyurethane had pyridine groups attached which formed complexes with metal salts. Films were then formed and subjected to a reducing agent in order to produce particulate metal filler. In this case the distribution of the filler which was formed was not uniform because the filler had tendency to aggregate (even though it was chemically attached to the matrix prior to the reduction). The following were factors controlling size and shape of these metal particles:

- The concentration of metal iron
- The morphology of polyurethane
- The polarity of the matrix

Polymeric segments could prevent excessive aggregation. These experiments show that there is no reasons to expect a polymer-filler system to have a homogeneous distribution. Even under such ideal conditions as described in the above two cases (the chemical affinity of substrates and the anchoring of the filler precursor) it did not occur. The general conclusion from these experiments is that a homogeneous distribution of filler in the matrix is rather the exception than the rule.

Studies on randomness of filler distribution in polymethylacrylate nanocomposite are interesting.[3] In this experiment, silica particles were formed both before and after matrix polymerization. The results indicated that the concentration of silica was a controlling factor in the stress-strain relationship rather than the uniformity of particle distribution. Also, there was no anisotropy of mechanical properties regardless of the sequence of filler formation. This outcome cannot be expected to be duplicated in all other systems. For example, when nickel coated fibers were used in an EMI shielding application.[4] When compounded with polycarbonate resin, fibers had a much worse performance than when a dry blend was prepared first and then incorporated into the polymer (Figure 7.1). In this case, pre-blending protected the fiber from breakage.

Calcium carbonate treated with stearic acid gave improved performance to poly(vinyl acetate) composites but only if the filler particles were sufficiently small.[5] Smaller particles tend to agglomerate if they are not coated. Coating prevents agglomeration and improves their interaction with the matrix. Large particles do not interact with the matrix but form defects in the composite. All three examples show that

- Uniform distribution of filler particles in a matrix does not guarantee improved performance
- At least two factors, filler surface availability and potential for interaction, contribute to improved filler distribution

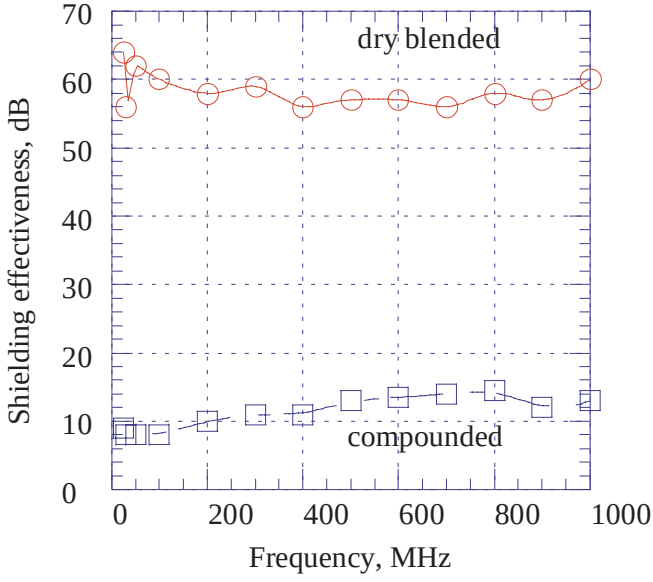

Figure 7.1. Shielding effectiveness. [Adapted, by permission, from Rosenov M W K, Bell J A E, Antec '97. Conference proceedings, Toronto, April 1997, 1492-8.]

Usually, a uniform distribution of the filler will give the most available surface for interaction. However, the nature of this surface has a strong influence on the properties of the filled material. In some applications, where perhaps thermal and electric conductivity improvements are sought, a uniform distribution will not necessary improve properties.

In thermoplastic melts, filler particles migrate due to a temperature gradient in the article during cooling. This produces an interphase tension at the particle-melt boundary. These forces cause particle movements from the cold regions into the melt.[6] Pressure sensitive adhesive containing fumed silica particles has a much lower tack on its surface than it has at the bottom of a cast film.[7] XPS analysis shows that the surface contains about 8 times more silicon than the bottom inferring that silica particles preferentially migrate to the surface.

The above systems are fairly simple, homogeneous systems since they contain only one polymer in the matrix. Blending polymers makes the behavior more complex. In polypropylene/polycarbonate blends, carbon black is preferentially located in the polycarbonate phase.[8] A blend which is better mixed is less conductive than a blend in which carbon black predominantly resides in the polycarbonate phase where it can form a conductive network. These are properties which control morphology (and related electric conductivity):

- Polarity
- Crystallinity
- Viscosity

These properties determine how carbon black will be distributed within the blend. These properties are not those of the filler but are the essential properties of the matrix. The matrix thus has strong influence on particle distribution. SEM studies showed that high vinyl polybutadiene and styrene-butadiene copolymers had morphologically identical carbon black distribution.[9] However, their mechanical properties were very different. NMR analysis indicated that the difference in mechanical behavior is related to the interaction and more precisely to the molecular motions in rubbery matrix.

The initial form of the filler is another complicating factor. Good and consistent dispersion of filler contributes to product properties. There two goals when filler is to be mixed:

- To reduce the size of filler particles (the intensity factor)
- To obtain a uniform distance between particles (the extensity factor)

The first determines property development, the second uniformity of these properties. Under the same conditions of mixing, the initial form of the filler plays dominant role. Consider carbon black. Pellets lose their initial shape during mixing process but are more difficult to disperse than non-pelletized blacks. Mixing can reduce the size of agglomerates but has much less influence on aggregates, and primary particles are not affected by mixing process. Filler form can affect product performance just as much as the intensity of processing (mixing).[10]

Filler particle distribution can be further complicated by the processing method since mixing is seldom last step of the process. Some classical examples are connected with the molding processes.[11-13] In the injection molding process, particles concentration around the gate axis increases as the mix passes the gate. Stream of particles is then diverted from the front surfaces towards the sides of the mold.[11] These phenomena cause the surfaces of injection molded parts to contain a lower concentration of filler particles than do their centers. The advancing surface contains increasingly more filler particles when the particle size is increased. This phenomenon produces two gradients of particle concentration. One in a plane perpendicular to the material flow (core-skin structure) with as a skin depleted of particles.[12] The other is along the flow direction with a higher concentration of particles close to the advancing front and a lower near the gate. Other effects are related to particle orientation in the matrix discussed below.[13]

We have outlined factors which affect particle distribution in a matrix. This distribution depends partly on filler properties but predominantly on the combination of properties of the pair filler-matrix. Filler distribution in a matrix depends on intended application. Some, such as applications which use fillers for reinforcement, require a homogeneous distribution of particles. In others, such as mentioned above electrical conductive materials, adhesives), a uniform distribution of filler particles may decrease their effectiveness.

7.2 ORIENTATION OF FILLER PARTICLE IN A MATRIX

Three aspects of orientation are considered here:

- How can orientation of filler particle be achieved?
- What kind of results can be expected?
- How does the orientation of filler particles affect material properties?

The simplest method of particle orientation involves material compression.[14] In an experiment, ferrite powders were dispersed in linear polyacrylamide, the gel was crosslinked, and the swollen gel compressed. This process resulted in particle orientation. Industrial processes, such as extrusion, injection, compression, and blow molding, fiber spinning, and thermoforming induce orientation due to flow.[15,16] Typical parameters which control fiber orientation in these processes include:

- Particle shape
- Filler concentration
- Viscosity of the matrix
- Rate of flow
- Shape and length of the die
- Length of the flow path in the cavity
- Thickness of the wall

Many other parameters may be involved depending on the method of processing. Such orientation not only occurs when processing from a solution or a melt but may also occur by inducing strain in the material.[15] Glass fiber reinforced polyamide-6 was subjected to such a strain. Heated specimens were extended under controlled strain and cooled under extension. Hencky strain was calculated from the following equation:

$$\varepsilon = \int d\varepsilon = \int_{L_o}^{L_f} \frac{dL}{L} = \ln\left(\frac{L_f}{L_o}\right) \qquad [7.1]$$

where:

ε	Hencky strain
L_o	initial length
L_f	length after extension

Fiber orientation was determined by microradiography. The images of microradiographs were digitized and their orientational distribution determined by image processing software. The fiber orientation function was calculated from the following equation:

$$J = 2\int_{-\pi/2}^{\pi/2} \cos^2\theta q(\theta) d(\theta) - 1 \qquad [7.2]$$

where:

θ	the fiber orientation angle
$q(\theta)$	the distribution of fiber orientation angles

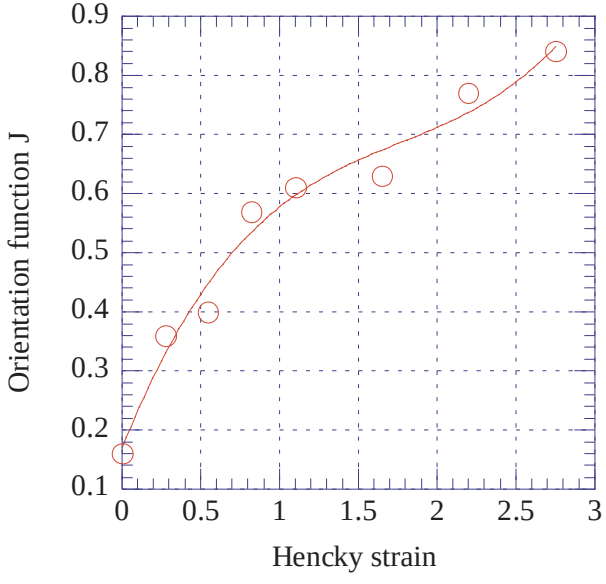

Figure 7.2. Orientation distribution function, J, vs. Hencky strain. [Adapted, by permission, from Wagner A H, Kalyon D M, Yazici R, Fiske T J, Antec '97. Conference proceedings, Toronto, April 1997, 996-1000.]

The fiber orientation function, J, equals 0 for random distribution and 1 for unidirectional distribution. Figure 7.2 shows the results obtained. This simple experiment shows that extension by ~1.5% causes a very high orientation of fibers (J = 0.84). The experiments show that a fairly large rate of flow is needed in the industrial processes to induce fiber orientation. For example, when the injection rate was increased from 6×10^{-8} to 1.7×10^{-7} m^3/s, the J value increased from 0.53 to 0.63 for HDPE filled with 20% glass fibers.[17] For the same conditions, the J value decreased from 0.53 to 0.32 when the gate diameter decreased from 3.2 mm to 1.7 mm. The maximum injection rate is limited by product requirement. For example, high speed injection of carbon fiber filled resin reduces electrical conductivity but improves appearance. It is necessary to find a compromise between appearance and conductivity.[18]

Shear controlled orientation technology was developed to optimize plastic properties by orientation of filler particles.[19] In this patented technology, the single feed is split into a plurality of feeds which can supply pressure to the mold cavity independent of the feed channel. Figure 7.3 shows feed arrangements. The shear is applied by a controlled movement of pistons which imposes microscopic shear. A perfect alignment of fibers can be obtained.

Fiber orientation can be induced by simultaneous shearing and application of electric fields.[20] Such conditions were simulated in a plate rheometer in which the plates were also inducing an electric field. Dielectric particles of filler were oriented in the same direction as that of the electric field. The time to reach an equili-

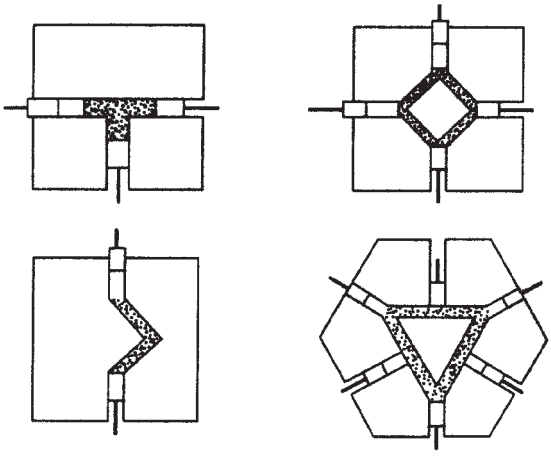

Figure 7.3. Feed arrangements to produce orientation of fibers. [Adapted, by permission, from Allan P S, Bevis M J, *Materials World*, **2**, No.1, 1994, 7-9.]

brated orientation was also measured. The 90% of all fibers aligned within 100 s. Exposure to magnetic field also produces orientation.[14]

These processes attempt to order particles in a predictable manner. How much orientation can be achieved? Figure 7.4 shows the effect of orientation of nickel fibers.[17] The graph shows that fibers are mostly aligned in the flow direction. The orientation was enhanced by an increased rate of flow but only for shorter fi-

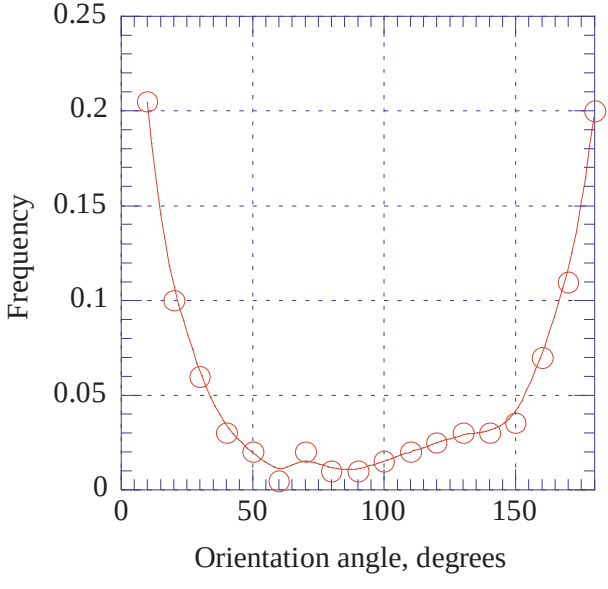

Figure 7.4. Fiber orientation distribution. [Adapted, by permission, from Fiske T, Gokturk H S, Yazici R, Kalyon D M, Antec '97. Conference proceedings, Toronto, April 1997, 1482-6.]

bers. The rate of flow did not have any effect on longer fibers (aspect ratio of 50). The distribution of fibers along a cross-section of cylindrical parts can take one of several forms.[16] Combinations of radial structure and onion-like structures can be distinguished. The core and skin have different structures. Increasing the concentration of filler increases the influence of the extrusion rate on the orientation of talc

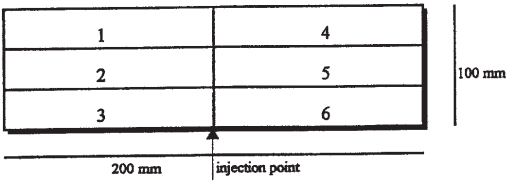

Figure 7.5. Longitudinal selection of test plate segments. [Adapted, by permission, from Barbosa S E, Kenny J M, Antec '97. Conference proceedings, Toronto, April 1997, 1855-9.]

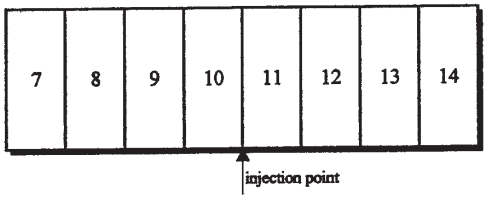

Figure 7.6. Widthwise selection of test plate segments. [Adapted, by permission, from Barbosa S E, Kenny J M, Antec '97. Conference proceedings, Toronto, April 1997, 1855-9.]

which as the concentration becomes greater than 20%, becomes more radially oriented with extrusion rate increasing.[16]

Also, the proportion of fibers in the skin (or shell) and those in the core depends on the rates of flow.[21] Low injection rates and low temperatures causes an expansion of the shell (skin) region.[22] These relationships also affect the orientation of polymer chains in filled and unfilled polymers during processing.[22] Orientation of fiber in blow molding of bottles filled with fibers caused anisotropy of properties. Tensile strength was increased in the machine direction.[23] At the same time, talc filled bottles had more uniform tensile properties than unfilled bottles.[24]

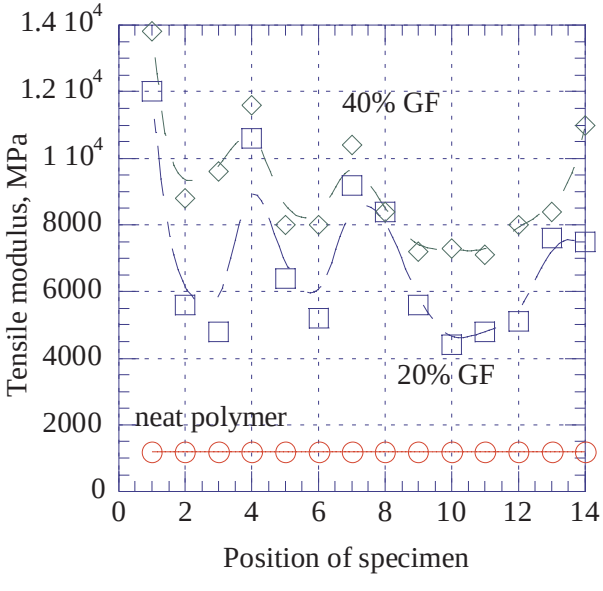

Figure 7.7. Tensile modulus of glass fiber reinforced polypropylene vs. position of sample. [Adapted, by permission, from Barbosa S E, Kenny J M, Antec '97. Conference proceedings, Toronto, April 1997, 1855-9.]

The distribution of fiber in an injection molded plate is shown in Figures 7.5 to 7.7.[25] Specimens for tensile testing were selected from injection molded plate as shown in Figures 7.5 and 7.6. Neat polypropylene has a low but consistent modulus throughout the width and length of the plate. The addition of fiber seems to increase the tensile modulus although readings were less uniform than expected. Fibers certainly travel preferentially with the front of injected material because the most distant segments have always the highest modulus. The lowest readings are from specimens close to the injection point. Increased concentration of filler adds to the uniformity of readings (more uniform readings for samples containing 40% fibers than for these containing 20% fibers). Blow molding of talc filled plastic bottles[13] and thermoformed talc filled thermoplastics produced materials which yielded similar test results.[26]

The relative magnetic permeability depends on the fiber orientation function, J (see Eq 7.2):

$$\mu' = \mu_o + 4J^2 \qquad [7.3]$$

where:

μ_o the relative magnetic permeability of a matrix filled with spherical particles of nickel

Figure 7.8 shows relationship between the relative magnetic permeability and the fiber orientation function.[17] The results came from an experiment previously discussed (see Figure 7.4).

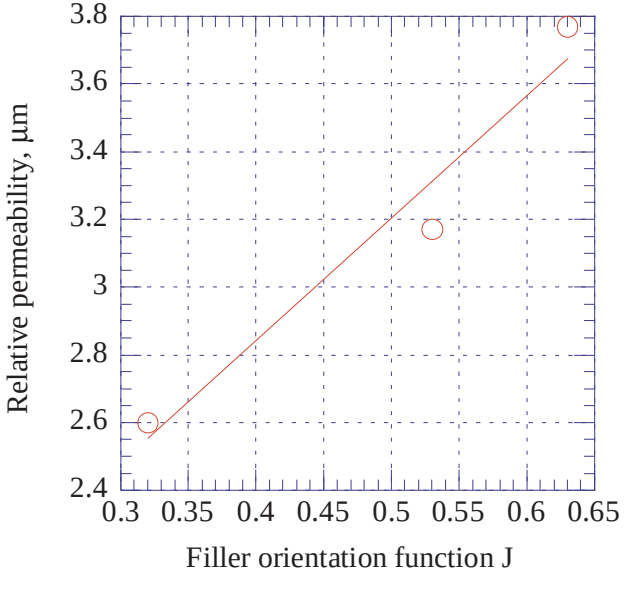

Figure 7.8. Relative magnetic permeability vs. fiber orientation function. [Adapted, by permission, from Fiske T, Gokturk H S, Yazici R, Kalyon D M, Antec '97. Conference proceedings, Toronto, April 1997, 1482-6.]

A polyamide gel filled with ferrite powder forms a ferroelastic material.[14] When the material is in a compressed state or in a magnetic field, filler particles are oriented. When the stress is released or the magnetic field is removed, particles become disoriented. When no stress is applied, material has no magnetic properties. Application of stress gives a measurable magnetic field (1-30 gauss) which depends on the extent of compression. When conditions are reversed, i.e. if material is put into a magnetic field it deforms to orient the filler. This is a good example describing memory of particles distribution and energy conversion (magnetic to mechanical and *vice versa*).

Fillers are known to affect UV stability of materials but little is known as to how the orientation of filler particles affects UV stability. Coatings and films designed with corrosion protecting barrier properties may contain dispersed mica or talc. The plates orientation prevents penetration of diffusing materials. To protect against UV degradation such a barrier would also be useful to exclude oxygen because photochemical changes are accelerated by oxygen. Until recently, there was little evidence that orientation of particles contributed to UV stabilization. A recent paper[27] seems to give experimental evidence that it does. Talc filled polypropylene test bars, prepared by injection molding, were exposed to UV radiation. Initial degradation of the filled material was faster than the unfilled control specimens containing filler but in longer exposure filled specimens were better protected and did not go through a further change on continued exposure. This may be explained by the fact that the material surface (the skin) did not contain many oriented particles, but internal core did. Therefore, the interior was protected by less a permeable barrier formed by the oriented particles of talc which did not allow oxygen to penetrate.

Figure 7.9 shows that orientation of fiber affects the wear resistance of a material.[28] The lowest wear occurs when fibers are perpendicular to the matting surface. If both matting surfaces are made out of fiber filled materials, the wear properties can be further optimized by the choice of fiber orientation in respect to both surfaces.

We have shown that orientation of filler particles can affect many properties (sometimes in unexpected ways). The best orientation depends on the property which is to be optimized and on the materials in the application. Extensive use is being made of these means of improving properties. Many materials can be further improved by application of these principles.

7.3 VOIDS

The term “void” may mean different things in relationship to filling and fillers. But all the meanings have one common denominator – they play a role in material reinforcement. A void may be

- An air filled space created around the filler particle by incomplete wetting or debonding

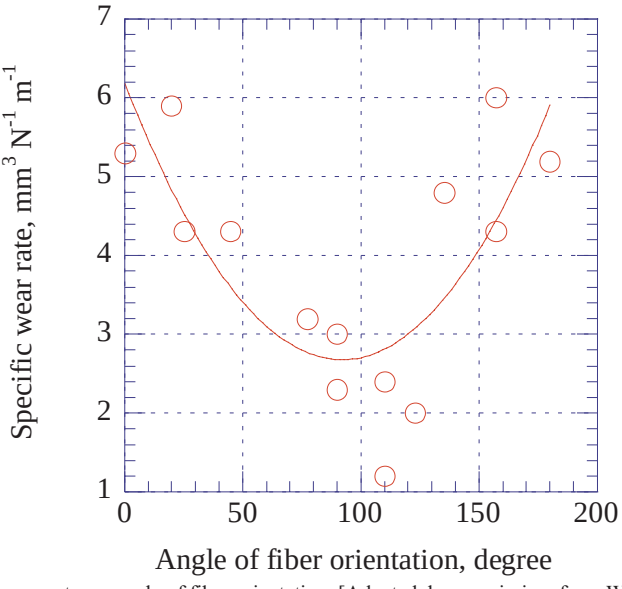

Figure 7.9. Specific wear rate vs. angle of fiber orientation. [Adapted, by permission, from Wada N, Uchiyama Y, Hosokawa M, *Int. Polym. Sci. Technol*., **21**, No.3, 1994, T/53-63.]

- An air bubble created in a filled material for the purpose other than toughening
- A very small air bubble (microvoid) created to toughen polymer
- The free space around filler such as carbon black or fumed silica which are characteristic of the structure of those materials

All these terms are used to explain various phenomena related to fillers.

A model was developed to estimate properties of polymer composites which have voids of various sizes (large and small).[29] Such voids are typically found between fiber tows (macrovoids) and inside the fiber tows (microvoids) in composites produced by liquid molding. The presence of these voids does prevent the matrix from adhering to the fiber which reduces the composite's mechanical performance. Larger voids do not seem to affect performance as much as smaller voids do. In practice, the volume of voids in normal production is within 5% of the total volume of the composite. At 5% void volume, the mechanical strength of composite can be reduced by as much as 30%. This is considered a substantial imperfection but it is found in practice. The model developed predicts values of mechanical properties which correlate with void volume. In another application, magnetic resonance imaging helped to determine voids in solid rocket propellants and liners similar to those used in space shuttle.[30] The voids were found to be in close proximity to the filler particles.

In the production of microporous sheets used as separation membranes, voids are internally created to make material permeable.[31] Polypropylene was highly

filled with calcium carbonate (~200% phr) and biaxially stretched. The stretching separates the matrix from the filler particles. This creates a soft membrane with gas and water vapor permeability (but liquid water does not penetrate the membrane). Changing filler content, particle size, and degree of stretching one can modify membrane properties. The degree of stretching is important because it determines mechanical properties in both directions of stretching. These properties can be optimized to give balanced tensile properties in both directions which is important in the practical applications of a membrane.

Void creation was simulated by mixing polystyrene with rigid particles.[32] This study was intended to develop an understanding of how impact resistance could be improved by incorporating voids rather than incorporating rubber. Addition of 1% rigid particles performed better than the impact modified resin. The optimum size of particles was ~2 μm. This effect is due to improvement in crack growth resistance due to shear deformation or crazing. An epoxy system was improved in a similar experiment but non-adhering organic particles were used to create microvoids.[33] Regardless of the particle type, at least a twofold improvement in fracture toughness was obtained.

Void volume is one of the main parameters used to characterize the structure of carbon black.[34-6] Void volume enters into the equation used to characterize interaggregate distance, IAD, as follows:

$$IAD = \frac{(1 - VV)}{(N_2SA \times \phi)} \qquad [7.4]$$

where:

IAD	interaggregate distance, nm
VV	void volume, cm^3/g
N_2SA	nitrogen surface area, m^2/g
ϕ	volume fraction

Void volume can be calculated using this equation after determining the surface area by nitrogen absorption (BET method) or by filling the voids with liquid. Typical values of void volume are 0.6-0.7 cm^3/g for carbon black and 0.5-0.97 cm^3/g for silica.

7.4 MATRIX-FILLER INTERACTION

Studies on filled systems all find that the experimental observations can be explained by matrix-filler interaction. This interaction is a complex process involving:

- A chemical reaction between the filler and matrix materials (Chapters 6 and 7)
- Physical interaction (van der Waals forces and hydrogen bonding)
- Changes in morphology of interacting components
- Mechanical interlocking

These processes modify surface layers of both interacting materials (filler and matrix) and form an interphase which differs in properties from the bulk matrix. The formation of the interphase is responsible for changes in the physical and mechanical properties of filled materials and usually improves material reinforcement.[37-47]

In ABS/glass beads system, thermo-physical measurements show that interaction between the ABS and the glass causes a decrease in heat capacity and increase in thermal conductivity due to restriction in molecular motions of the resin surrounding glass beads.[37] Molecular transformations in the vicinity of filler particles is a local phenomenon dependent on the concentration of filler particles.[39] At low loadings (10% and below), the particles are surrounded by a tightly bound polymer covered by a layer of loosely bound chains. As the loading increases, the areas of loosely bound polymer begin to overlap, consisting the entire matrix to be influenced by the filler. If filler loading is high, there is little space left for loosely bound polymer and the participation of the layers of tightly bound polymer increases. At different filler loadings, a change in the interaction mechanism is likely to occur.

Particle-particle interaction affects maximum particle packing and it is influenced, in turn, by surface coating of the filler.[41] Packing density of the filler is not a simple geometrical phenomenon. It depends on interaction with the matrix. This interaction changes the morphology of matrix.[43] Adhered layers of polymer have a different conformation from polymer in the crystalline structures formed due to the polymer crystallization. The character of filler determines the conformation of the surrounding polymer and therefore strongly influences mechanical and chemical properties. In many filled systems, a second glass transition temperature can be detected due to the presence of adsorbed layers on the surface of filler.[44]

These and other phenomena are the subject of discussion in the following sections of this chapter.

7.5 CHEMICAL INTERACTIONS

Chapter 6 discussed chemical reactions which occur on the surface of the filler and with the filler surface. Now we focus on how the interphase is created and on how interface chemistry affects the formation of interphase.

Figures 7.10 to 7.12 show three models of interaction between the surface of the filler and the matrix.[35,39,48] Each model was developed to examine interaction in different system. They complement each other and show the complexity of interaction. The models also help us to distinguish between chemical and physical interactions.

This model was mentioned in the previous section.[39] An increase in the amount of filler decreases the average particle distance. When a relatively small number of particles is present (7.10A), particles influence the surrounding matrix but there is enough available bulk which is not subject to interactions with the filler surface (line-shaded areas are particles of filler, black areas correspond to the

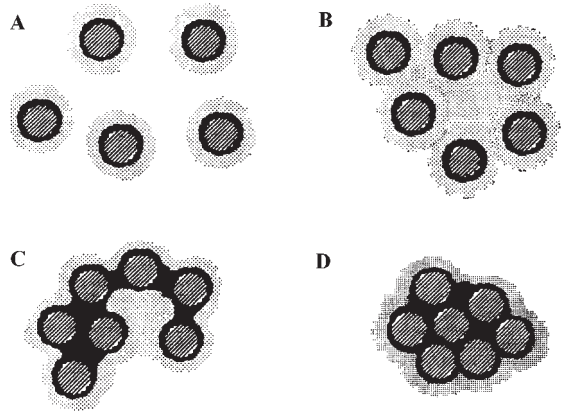

Figure 7.10. Schematic model of morphological transformations in filled polymers. A - silica content less than 10 wt% ($d>d_{cr}$), B - silica content ~10 wt% ($d=d_{cr}$), C - silica content ~20 wt% ($d<d_{cr}$), D - silica content over 50 wt%. [Adapted, by permission, from Tsagaropoulos G, Eisenberg A, *Macromolecules*, **28**, No.18, 1995, 6067-77.]

tightly bound resin, gray areas to loosely bound resin). There is only one glass transition. This indicates that the mobility of polymer next to the immobilized layer is not significantly affected. The magnitude of the first glass transition does decrease indicating that some polymer is involved in the formation of tightly bound layers. When the concentration of particles becomes close to critical, d_{cr}, the mobility of all chains in the composite becomes affected (7.10B). At this point, the second glass transition temperature can be detected, signifying formation of a substantial amount of loosely bound polymer. As more filler particles are incorporated (7.10C) more of the polymer becomes tightly bound pretty much in amount proportional to the increase in filler concentration. The second glass transition temperature becomes less easy to detect. At high concentration of filler (7.10D), most of the polymer is immobilized. The conclusions from this model are:

- Tightly and loosely bound polymer are two distinct and different physical materials
- Filler-matrix interaction affects chain mobility
- Chain mobility is controlled by the concentration of filler

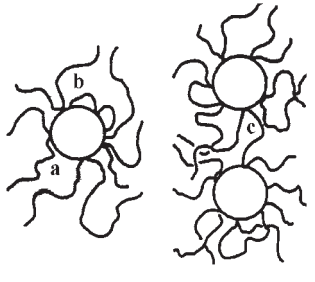

Figure 7.11. The concept of segmental interaction with a carbon black surface. [Adapted, by permission, from Wolff S, *Rubb.Chem.Technol*., **69**, No.3, 1996, 325-46.]

The second model shows us how chains can get attached to the surface of carbon black (Figure 7.11).[35] The chain can be attached at single point (a), at more than one point (b), or the chain can bridge two or more filler particles (c). This model does not indicate if a chemical reaction is involved but it can be anticipated that, since reactive functional groups can be positioned in the middle of chain or at its ends, the reactions may involve chain segment or terminal group. It might be thought that both models complement each other by showing that the probability of particles bridging increases with filler concentration. In rubber, a gel is formed

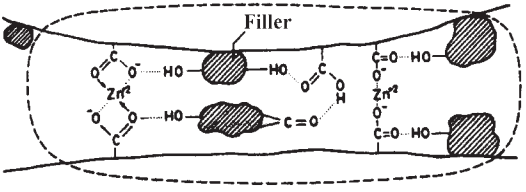

Figure 7.12. A mechanism of interaction between filler and ionic groups in the restricted mobility region in EPDM. [Adapted, by permission, from Datta S, De S K, Kontos E G, Wefer J M, Wagner P, Vidal A, *Polymer*, **37**, No.15, 1996, 3431-5.]

but only when configuration (c) occurs (two or more particles are connected).

Figure 7.12 depicts a model of chemical interactions proposed for a system of carbon black and maleated EPDM.[48] There are two types of links. Hydrogen bonding and covalent bonding which is characterized by the attachment of filler particles to the chain. Because the rubber is crosslinked there is more opportunity for it to form interaction.

This system follows the Guth and Gold equation:

$$\frac{E'_f}{E'_g} = 1 + 1.3\phi + 14.3\phi^2 \qquad [7.5]$$

where:

E'_f storage modulus of filled system
E'_g storage modulus of unfilled rubber
ϕ volume fraction of filler

The Eq 7.5 shows that the degree of reinforcement (which correlates to the ratio of the storage moduli) increases with increasing filler concentration (similar to the first model (Figure 7.10)). A second glass transition temperature is not detected but tanδ decreases as the concentration of filler increases indicating that the number of crosslinks increases. It is interesting to analyze the numerical values of coefficients at the right side of Eq 7.5. The Guth and Gold equation such as Eq 7.5 has the following general form:

$$E'_f = E'_o(1 + \alpha\phi + \beta\phi^2) \qquad [7.6]$$

α coefficient which depends on filler dispersion
β coefficient which depends on molecular interaction

For van der Waals interaction, $\alpha = 2.5$ and $\beta = 14.1$. For the system containing carboxylated acrylonitrile rubber and ISAF carbon black, $\alpha = 4$ and $\beta = 42$. If ISAF carbon black is oxidized, α remains the same and β increases to 53 which is consistent with the fact that oxidized carbon black has more reactive sites and therefore molecular interaction should increase.[49] When the system is vulcanized, β further increases to 62 for ISAF carbon black and to 68 for oxidized carbon black, meaning that additional interactions occur. Additional mixing also increases the value of α. This is what mixing is intended to do. Because mixing increases the

value of α beyond what is considered typical of van der Waals forces, it plays an essential role in promoting chemical reactions.

Ayala *et al*.[50] proposed the following equation to describe rubber-filler interaction:

$$I = \sigma / \eta \qquad [7.7]$$

σ the slope of stress-strain curve in the relatively linear region
η filler-filler networking parameter calculated from ratio of storage modulus at high and low strains

This equation implies that reduction of filler-filler interaction increases rubber-filler interaction which is what mixing does. Figure 7.13 confirms the usefulness of equation 7.7.

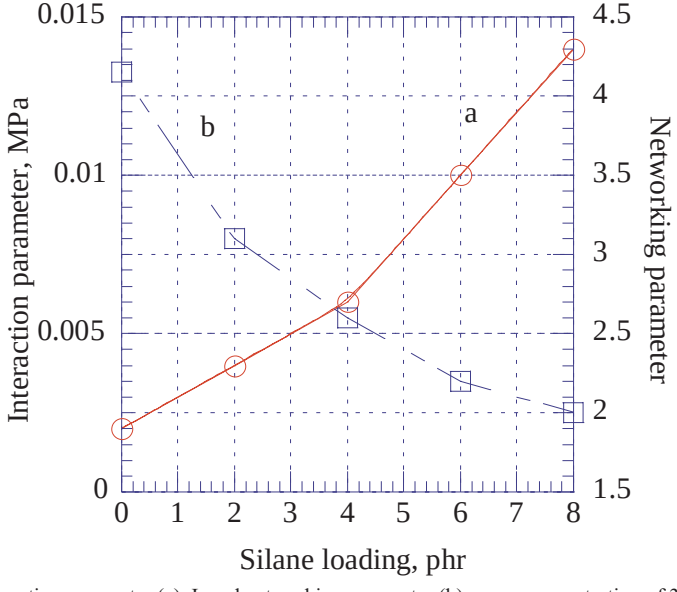

Figure 7.13. Interaction parameter (a), I, and networking parameter (b), η, vs. concentration of 3-aminopropyltriethoxysilane in NBR-carbon black system. [Data from Bandyopadhyay S, De P P, Tripathy D K, De S K, *J. Appl. Polym. Sci*., **61**, No.10, 1996, 1813-20.]

Silane is added to increase bonding between rubber and filler. The experimental results show that the physical interaction between filler particles is decreased and chemical bonding is increased. Other papers by the same research group show similar trends for other systems.[52,53] Several research methods are used to identify the exact nature of chemical interactions.[54-57] ^{1}H magic-angle spinning NMR, IR, Raman, and ESCA are the most successful techniques used for these purposes.

This left us conclude that:

- The effect of chemical sites on the filler surface should be interpreted in the context of the sphere of influence of chemical interactions

- This sphere of influence includes the nature of chemical bonding, properties of the formed structure, and the concentration of filler particles
- An increase in filler concentration alters the mechanism of interaction and the interaction influences the properties of the materials
- The methods of measurement can distinguish between chemical bonding and physical interaction.

7.6 OTHER INTERACTIONS

The interactions other than the formation of covalent bonds include:

- Van der Waals forces
- Ionic interactions
- Hydrogen bonding
- Acid-base interaction
- Mechanical interlocking
- Other interactions

Van der Waals forces are made up of:

- Dispersion forces (London)
- Orientation forces (Keesom)
- Induction forces (Debye)

The dispersion force is the major factor in non-chemical interaction. London derived an equation characterizing dispersion energy for attracting two spherical molecules:

$$E_d = -\frac{3}{4}\left[\frac{1}{(4\pi\varepsilon_o)^2}\right]\left(\frac{I\alpha^2}{r^6}\right) \qquad [7.8]$$

where:

ε_o permittivity in free space,
I ionization constant,
α electronic polarizability of molecule,
r separation distance.

The London theory was later modified to account for retardation effects occurring at greater separation distances:

$$E_r = -\left[\frac{1}{(4\pi\varepsilon_o)^2}\right]\left(\frac{\alpha^2}{r^6}\right)\left(\frac{hc}{r}\right) \qquad [7.9]$$

where:

h Planck constant,
c light velocity.

Dispersion forces act over long separation distances (from interatomic distance to 10 nm and above) and are affected by nearby bodies. These forces align and orient molecules. Powerful as they are, dispersion forces do decrease rapidly as the separation distance between two interacting bodies increases. The energy is inversely proportional to the sixth or seventh power of separation distance. Electrons traveling around the nucleus form an asymmetric charge distribution

which produces a dipole which generates short-lived electric fields which, in turn, induce dipoles in the neighborhood. Dipoles are attracted by each other and this is what generates the force of dispersion.

Keesom analyzed the effect of the orientation of dipoles on the energy of interaction between the molecules:

$$E_o - \frac{2}{3}\left[\frac{1}{(4\pi\varepsilon_o)^2}\right]\left(\frac{\mu_1^2\mu_2^2}{kTr^6}\right) \qquad [7.10]$$

where:

μ	dipole moment,
k	Boltzmann constant,
T	absolute temperature

Note that temperature is a parameter of the equation. As the material temperature rises during processing, the value of orientation energy becomes negligible. In a typical system conflicting dipole fields are created which significantly reduce dipole-dipole net interaction. Keesom forces, unlike London forces, do not apply to nonpolar substances because both dipoles, which participate in the interaction, must be permanent dipoles (London forces do not require the presence of permanent dipoles).

Debye modified the Keesom equation to account for experimental observations. He showed that the energy of interaction was not as greatly reduced by temperature as was predicted by the Keesom equation:

$$E_i = \left[\frac{1}{(4\pi\varepsilon_o)^2}\right]\left(\frac{\alpha_1\mu_2^2 + \alpha_2\mu_1^2}{r^6}\right) \qquad [7.11]$$

This equation gives the induction energy for dipole-induced dipole interaction; for dipole-nonpolar, $\alpha_1\mu_2^2$ is neglected.

London dispersion forces account for more than 75% (up to as much as 100%) of total interaction energy. Very polar small molecules such as water are an exception. These owe most of their interaction energy to hydrogen bonding (only 24% of the attractive forces are contributed by dispersion interaction). Particle size plays a very important role. Over large distances, the attractive forces between particles, since it is inversely proportional to the seventh power of the separation distance, become negligible. Van der Waals forces are at least a few hundred times lower than that of covalent bonds but are strong enough to cause difficulties in the dispersion of some grades of carbon black so that the desired increase in tensile strength, due to the reinforcing effect, is not achieved. The type of interacting material is also important. Molecules prefer to interact with molecules of their own kind and the hydrophobic-hydrophilic effect is significant.

The equation for van der Waals forces as applied to particle interactions was developed by Hamaker:[5]

$$F = \frac{A_1}{6}d_2(d+t)\left(\frac{1}{a^2} + \frac{1}{b^2} + \frac{2}{ab}\right) \qquad [7.12]$$

where:

A_1	Hamaker coefficient,
d	diameter of two equal spheres,
t	separation distance between two spheres,
a	$= t^2 + 2dt$,
b	$= a + d^2$.

The Hamaker coefficient is the sum of three terms: London, Keesom, and Debye. His equation is an integration of the forces acting between a pair of particles across the phase boundary. Hartley[58] found that Hamaker's constant for carbon blacks is in the range of $0.6\text{-}5.8\times10^{-19}$ J, which is in agreement with the literature and theory. Van der Waals forces play a significant role in carbon black dispersions, but not in the dispersion of titanium dioxide. Titanium dioxide has an adsorbed layer of moisture, which not only reduces van der Waals forces but causes a liquid bridging force that dominates flocculation. Thus, the cohesiveness of both carbon black and TiO_2 depends, on entirely different principles.

This theoretical work was utilized by Good and Fowkes who developed theories relating van der Waals forces to surface tension and to the work of adhesion. These concepts are discussed in Chapters 5 & 14.

Ionic interaction is believed to play a role in the reinforcement of EPDM crosslinked by ZnO with modified silica particles.[59] A restricted mobility region is formed by ionic aggregates. In other work, muscovite mica was modified by various cations.[60] Polymers with crown ethers were absorbed on such modified mica. It was discovered that the ionic radius was an important parameter in the absorption process. Radii in the range of 130-150 pm (K^+, Rb^+, and Ba^{2+}) were optimum for absorption. Ionic forces are equivalent to covalent bonding forces. The highest energy is attained when two interacting ions are in close proximity, i.e., separated by the length of typical bond. If the distance of separation is larger than the bond length, the energy of interaction rapidly decreases.

Covalent forces binding atoms in molecules range from 200 to 900 kJ/mol. The energy of hydrogen bonding is in the range of 8 to 42 kJ/mol which is small compared with covalent bonding force but considerably higher than that attributed to van der Waals interactions. Because of the relatively low energy required for bond formation and breaking, hydrogen bonding plays an important role at room temperature. It has an essential effect on interaction between surfaces of inorganic materials which contain hydroxyl groups on their surface and organic molecules present in their proximity. Silicone rubber reinforcement is an example of hydrogen bonding which has an increased apparent crosslink density.[61] Figure 6.25 shows how silica loading increases ΔL (apparent crosslink density). Here, two forces, hydrogen bonding and polymer absorption on the surface of silica particles, are responsible.

The acidity or basicity of a solid surface is determined by its isoelectric point, I_s. Water is basic on an acidic surface and acidic on a basic surface. The measure of bond energy is given by the equation:

$$\Delta H \cong \frac{DN \times AN}{100} \qquad [7.13]$$

where:
DN donor number
AN acceptor number

Acid-base interaction affects the mutual interaction between a solid (e.g., filler) and a liquid (e.g., solvent, polymer, etc.), as well as between a liquid and a liquid. This type of interaction may also affect the conformation of the polymer molecule when it is in contact with another acceptor/donor. More information on acid-base interaction is included in Chapters 5 and 14.

Mechanical interlocking is commonly thought of a macroscopic phenomenon in the adhesion between a substrate and an adhesive. But the interaction between polymer and filler plays a role and is elegantly exemplified in the rubber-silica system.[62] The authors[62] investigated the size of voids in fumed silica in its original form and after compounding with rubber. Pore size in the original silica was determined by a mercury porosimeter. After the silica was compounded with rubber the silica pores were cleaned by pyrolizing the rubber at 480°C. The pore sizes were measured again using the mercury porosimeter. It was also determined that the pyrolysis conditions do not affect the pore size of silica. It was found that the silica grade which caused the most reinforcement of rubber had widened pores after it was compounded. The increase in the size of pores depended on the conditions of mixing and on the formulation of rubber. Reinforcement required the initial size of silica pores to be large enough to allow penetration by rubber chains.

There are other interactions. The surface of carbon black has a tri-dimensional structure dependent on the conditions of its preparation. The rubber chains are thought to fit into imperfections in the surface and produce reinforcing effect.[63] In another paper, the reinforcement effect was correlated with surface roughness.[64] This paper postulated that the chains align themselves over the uneven surface to cause reinforcement.

Another interaction is responsible for the recovery of the material after it is subjected to stress.[65] Rubber bridging the neighboring particles of filler is an example. Some particles are connected through several rubber chains which makes their association more permanent and assures filler-filler contact. These filler-filler contacts are responsible for the recovery since, unlike chain-filler contacts, they store the strain energy which is then used in the recovery process. Chain-filler contacts can easily debond or rearrange in different location and this process does not result in recovery of the initial shape.

A study of paint technology reveals other interactions.[66] The layer of paint in immediate contact with the surface of the substrate is depleted of filler. The next layer is enriched with filler. Between the last layer and the bulk of paint there is still polymer-rich layer. This effect is attributed to the affinity of the polymer with the substrate. This affinity leads to polymer migration. It also causes binder orientation

which leads to the increased interaction with filler. This in turn, causes migration of filler particles from adjacent layers.

Polymers filled with ultrafine metal particles form periodic stripes.[67] These stripes are thought to be caused by an inhomogeneous electric field which induces electrostatic interactions among the polarized polymer chains. The phenomenon is known as mutual dielectrophoresis.

Thus, many complex phenomena can affect the organization of the interface and this, in turn, affects how fillers contribute to the reinforcement.

7.7 INTERPHASE ORGANIZATION

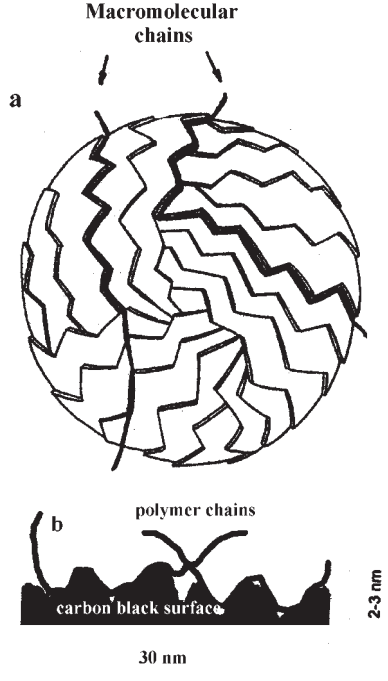

Figure 7.14. Conformation of a chain on the surface of carbon black. (a) direct view of surface, (b) cross-section through the surface. [After refs. 63, 64.]

Carbon black research[63-65,68,69] focused on a study of the structure at the interface and attempt to explain reinforcement. More recently, other fillers have been investigated.[66,70-75] A variety of surface structures have been postulated for carbon black to explain the organization at the interface.[63] Figure 7.14 gives examples of how the surface of a filler can contribute to interface organization.[63,64] The attachment of chain to the surface of the filler is accomplished through a process called "wetting" and its removal through a process of "dewetting". Chains which are removed from the surface by strain can become attached again which is consistent with some mechanisms of reinforcement (e.g., molecular slippage).

Another concept of the structure at the interface has been proposed to overcome some of difficulties associated with the previous model (Figure 7.15).[65] In this model, a distinction is made between two types of contacts. FF is filler-filler contact and FM is filler-matrix contact. Special emphasis is given to the contact FF which is believed to explain energy storage during strain. The

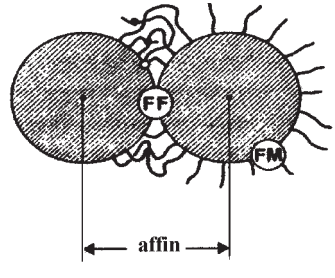

Figure 7.15. The basic reinforcing component. [Adapted, by permission, from Strauss M, Pieper T, Peng W, Kilian H G, *Makromol. Chem., Macromol. Symp.*, **76**, 1993, 131-6.]

contact FF is well protected by surrounding bonds. The separation of filler particles is limited to a certain distance when the strain is less than a critical. This allows to store energy due to the action of the van der Waals and the elastic forces of the protecting chains.

The polymer chains are not the only components of the mixtures which are capable of interacting with the filler surface. Other additives can be adsorbed on the surface to create a situation in which monolayer or multilayer coverage competes to form an association with the surface.[69] Such coverages contribute to the organization of interface. The first layer of adsorbed components in the formulation has an impact on the entire organization of the interphase because it affects configuration of adsorbed chains and the crystallization processes around the adsorbed layer.

Investigations of polymer blends has developed an increased understanding of interphase organization. In blends two interfaces exists: the interface between two matrix types and distribution of filler and its interfaces with this matrices. The interphase of carbon black in blends of natural rubber and EPDM depends on the character of carbon black (surface groups available for interaction), the viscosity, the molecular weight, and on the order of mixing.[68] These organizations determine the mechanical properties of rubber for tires.

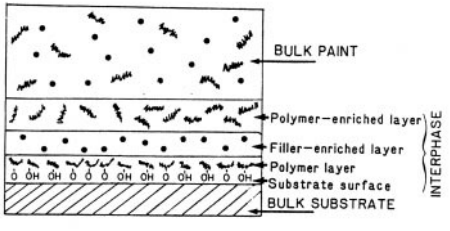

Figure 7.16. Interphase between paint and substrate. [Adapted, by permission, from Roche A A, Dole P, Bouzziri M, *J. Adhesion Sci. Technol*., **8**, No.6, 1994, 587-609.]

Figure 7.16 shows interface formation with painted substrate.[66] The mechanism of organization was discussed in the previous section. The alignment in the polymer layer plays a large part in polymer-filler interaction in the adjacent layers. The way in which polymer is configured on the substrate surface determines if polymer chains are readily available for interaction with filler. This example shows that it is not only the filler and the matrix which play a role in the interphase organization.

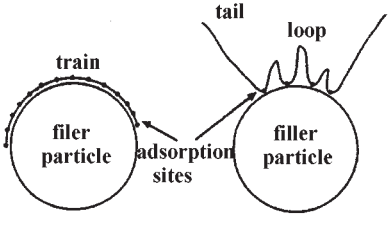

Figure 7.17. Polymer chain absorption onto a solid surface. [Adapted, by permission, from Hedgus C R, Kamel I L,US, J. Coatings Technol., 65, No.821, June 1993, 49-61.]

In Figure 7.17, we have two chain adsorption methods on the surfaces of silica or titanium dioxide.[70] On larger particles, the chain assumes a flat coverage of the surface (train). On smaller particles, the curvature of surface does not allow for train configuration. Instead, loops and tails are formed. In the first case, the interphase is thinner than in the second and

Figure 7.18. Optical micrograph with crossed polars of bamboo fiber in maleated polypropylene. [Adapted, by permission, from Mi Y, Chen X, Guo Q, *J. Appl. Polym. Sci*., **64**, 1997, 1267-73.]

fewer chains participate in the formation of the interface. On the other hand chain configuration is different in both cases.

Figure 7.18 shows how crystalline structure is affected by the presence of fiber. Here, bamboo fiber was used for polypropylene reinforcement.[71] A nucleation occurs on the surfaces of fiber. Spherulites grow from the fiber surface. Such growth results in transcrystallinity. The maleation of polypropylene increases interaction because of reactivity with OH groups on the fiber surface. This organization contributes to the reinforcement.

Glass fibers sized with polyurethane and polyvinyl acetate formed different interfaces. This was due to the differences in reactivity and miscibility. Polyurethane forms a stronger interface because it is reactive and miscible with epoxy resin.[74] Surface tension of glass surface in a molten state correlates with the interface formation with polymer.[75] The diffusion at interface contributes to a complex structure controlling properties of the interphase. The analysis of the diffusion at the interphase has helped to develop an understanding of the formation of metal-polymer interfaces and plastic welding.

In summary, numerous effects influence interphase formation. The most important influences depend on the type of active groups on particle surface, particle size, surface shape, and interaction with the matrix. The interphase can be modified by mixing process, the order of addition, filler concentration, and the orientation of the chains on the surfaces among other possible causes of interphase modification.

7.8 INTERFACIAL ADHESION

Interfacial adhesion can be predicted from available models or from data on the mechanical performance of filled systems.[5,76-9] The following equation describes the reversible work of adhesion:

$$W_{AB} = \gamma_A + \gamma_B - \gamma_{AB} \qquad [7.14]$$

where:

γ_A and γ_B surface free energies of adhering substances
γ_{AB} interfacial energy

The interaction depends on the morphology and the chemical structure of both the filler and the matrix. The condition which outlines the limit of the stress, which the bonding can withstand, is determined from the following equation:

$$\sigma^D = -C_1\sigma^T + \sqrt{\frac{C_2 W_{mf}}{R}} \qquad [7.15]$$

where:

σ^D	dewetting stress
σ^T	thermal stress
C_1, C_2	constants
W_{mf}	work of adhesion between matrix and filler
R	average radius of filler particles

The dewetting model is useful in predicting critical stress from a knowledge of tensile yield stress.[5] The results of tensile testing can be used to predict adhesion of polymer to filler particles of different sizes. The following model is useful for this purpose:

$$\sigma_c = \sigma_p(1 - a\Phi_f^b + c\Phi_f^d) \qquad [7.16]$$

where:

σ_c	tensile strength of composite
σ_p	tensile strength of polymer
a, b, c, d	coefficients
Φ_f	volume fraction of filler

Coefficient "a" is related to stress concentration. Coefficients "c" and "d" are related to the adhesion of the polymer matrix to filler. In an experiment involving different sizes of calcium carbonate in poly(vinyl acetate), small and medium particles had a much larger values of coefficients "c" and "d" than did large particles. This is in agreement with an experiment which shows that large particles decrease the mechanical properties of composites.

Interfacial adhesion can also be estimated from the Suetsugu-Sakairi equation:[80]

$$\sigma_c = K\Phi\chi V_f + \sigma_m(1 - V_f) \qquad [7.17]$$

where:

σ_c	composite strength
K	coefficient reflecting the orientation and the length distribution of glass fiber
σ_m	matrix strength
Φ	interfacial adhesion parameter
χ	glass fiber aspect ratio
V_f	volume fraction of glass fiber

This equation was used to estimate the interfacial adhesion in comparison with the acid-base properties of glass fibers in LDPE.[79] The effect of surface treatment of glass beads on their interfacial adhesion to PET was also estimated from a mechanical property measurement.[78] A mathematical model describing the adsorption of polymers on filler surfaces related coupling density to the average area available for coupling between rubber and filler surface.[76]

7.9 INTERPHASE THICKNESS

Several methods are used to determine the thickness of the interphase.[70] Table 7.1 lists the most important methods and the results of the thickness of an interphase

obtained from several sources. The equation below gives the correction parameter, B, in relationship to the matrix-filler interphase:[81,82]

$$B = (1 + \Delta R / R)^3 \qquad [7.18]$$

where:
ΔR effective thickness of interphase
R average radius of filler particles

Table 7.1. Interphase thickness

System	ΔR, nm	R, nm	ΔR/R	Method of determination	Refs.
Natural rubber/silica	5.2	8.7	0.60	DMA	83
SBR/silica	4.0	7.9	0.51	DMA	83
NBR/silica	3.7	8.0	0.46	DMA	83
Immobilized layer	0.5-2			general range	39
Restricted mobility	2.5-9			general range	39
Rubber/carbon black (CB)	10				84
Immobilized layer	0.4-1.3			range for rubber/CB	45
Restricted mobility	3-6.6			range for rubber/CB	45
PMMA/TiO_2	70	150	0.47	viscosity	70
PMMA/TiO_2	65	96	0.67	viscosity	70
PMMA/TiO_2	51	73	0.63	viscosity	70
PMMA/silica	17	8	2.18	viscosity	70
PMMA/glass	1.4	18	0.08	viscosity	70
PMMA/mica	0.11	0.75	0.15	viscosity	70
PS/glass	1	20	0.05	viscosity	70
PS/mica	0.06	0.66	0.09	viscosity	70
PVA/PS particles	0.24	3	0.08	ultracentrifuge	85
Elastomer/carbon black	0.13	2.2	0.06	bound rubber	86

This equation includes the parameters used in Table 7.1 to characterize the interphase thickness. The results presented are much affected by the method of measurement. The methods of measurement are indirect therefore it is quite difficult to estimate what the potential error of measurement may be. There are

some data in the literature (not included here) which show thicknesses several orders of magnitude higher than the results presented in the Table 7.1. There is a need for further studies to give credible values of the interphase thickness which are necessary to establish other related properties of filled materials such as effective filler volume, bound rubber, reinforcement, etc.

The thickness of the interphase depends on the reactivity of the filler surface with the matrix material. It also depends on their physical affinity.[87] Increased acid-base interaction between chlorinated polyethylene and titanium dioxide increases the thickness of the adsorbed layer. There is a maximum of thickness of interphase which depends on the properties of polymer bulk. The acid-base interaction is more dependent on how the filler is modified than on the matrix properties themselves. Both filler and matrix are responsible for the formation of an equilibrium, although each contributes in a different way.

7.10 FILLER-CHAIN LINKS

Here, a distinction is made regarding the "permanence" of filler chain bonds. This subject has evolved throughout this chapter and it is an important factor in understanding the mechanism of reinforcement.

Chains arrive at the filler's surface at different time scales. The early arriving chains can select any part of the free surface and have an increased probability of forming consecutive links with other points on the surface after forming an initial contact point. This process continues until most of the available sites are occupied. The chains which arrive first have a high probability of forming strong links because they can be either attached at several segments along their length or form a "train" configuration which involves many neighboring segments of the same chain. Latecomers find the filler surface mostly occupied by existing links. The probability of their forming stable links is severely reduced because only a few isolated sites are available. These chains can be removed from the surface more easily than chains with more permanent linkages. In crosslinked systems, the total network developed can be expressed by the following equation:[88]

$$N = N_c + N_{st} + N_{un} \qquad [7.19]$$

where:

N_c	chemical network density
N_{st}	network formed by stable links
N_{un}	network formed by unstable links

This equation gives a quantitative description of the storage modulus of a filled material:

$$G'(\gamma) = (N_c + N_{st} + N_{un}(\gamma))kT \qquad [7.20]$$

where:

$G'(\gamma)$	storage modulus dependent on γ

γ deformation amplitude
k Boltzmann constant
T temperature

Equation 7.20 shows that the changes in mechanical properties are first affected by temperature and then by the network of unstable links. Only after the unstable links are consumed stable links take the impact of changes occurring in the material. A similar logic can be applied to show that filler concentration also plays an essential role, considering that with small addition of filler most chains will form weak bonds because of very high competition for free surfaces on filler particles and the effect of reinforcement will be diminished. This is expressed by a simple equation:[89]

$$\gamma_{n,B} = 1 + \gamma_n \qquad [7.21]$$

where:
$\gamma_{n,B}$ number of adsorbed segments per chain
γ_n adsorption index

When filler concentration is low, $\gamma_{n,B} \approx 1$. Each filler is bound only once. Carbon black filled rubber does not form gel if only small amounts of carbon black are used. The molecular weight of polymer in the matrix affects the fraction of bound polymer according to the equation:[90]

$$\phi_B = \phi_M (1 - \phi_M / 4) \qquad [7.22]$$

where:
ϕ_B fraction of bound polymer
ϕ_M $= M_n^{1/2}$ maximum fraction of polymer which can be bound

As molecular weight increases, ϕ_B increases as does the probability of multiple connections.

7.11 CHAIN DYNAMICS

Section 6.11 is devoted to molecular mobility and, in it, the properties of macromolecular chains in filled systems are discussed. This section includes a brief evaluation of chain dynamics in relationship to "weak" and "strong" bondings of polymer chains which were introduced as a concept in the previous paragraphs.

Based on NMR studies, which play a prominent role in clarifying the mechanisms of interaction, monomeric units (or interacting segments) can be divided into three groups:[90]

- Those fixed on the surface – magnetic interactions of protons attached to these monomeric units are strong and the relaxation process is characterized by a high relaxation rate, σ_B. These units behave in a manner similar to the units of polymer in a glassy state.

- Forming loops and tails – these monomeric units have the freedom of a random rotation. Conformational fluctuations are restricted by fixed points on the filler's surface. The relaxation rate of these units, σ_L, is reduced according to the equation: $\sigma_L = \sigma_B / < n >$; where <n> is the mean number of skeletal bonds in one loop. With this relationship the relaxation rate decreases with the number of units in the loop. These units behave in a manner similar to polymer gels.
- Free chains – these units have the freedom of motion typical of an unfilled matrix. Their relaxation rates, σ_F, are given by the following equation: $\sigma_F = \sigma_B(\sigma_B \tau_c)$; where $\sigma_B(\sigma_B \tau_c)$ is a reduction factor related to τ_c which is the mean correlation time of random motions involved in the dynamics of the chain.

The importance of this classification is in characterizing the dynamics of diffusional processes and the strength of topological constraints to which the monomeric units (chain segments) are exposed.

NMR determines two types of spin-spin relaxation times: short, T_{2s}, and long, T_{2l}, which are for tightly and loosely bound polymer, respectively.[83] From modification studies of silica particles, it has been found that silanol groups are the main factor in increasing T_{2s}. Any reduction in silanol group concentration results in an increase of T_{2l} and a decrease in T_{2s}. This is in accordance with the logical prediction of the behavior of such system. Computer simulations of networks in conjunction with experimental studies gives further insight into the chain dynamics in filled systems.[91]

7.12 BOUND RUBBER

Bound rubber is the fraction of polymer which is not extracted by a good solvent from a rubber-filler mix. It is a measure of rubber reinforcement as well as of filler activity towards the rubber. This concept was introduced in 1925 by Twiss.[92] Although, the traditional term "bound rubber" is commonly used for rubber compounds, the concept can also be applied to other macromolecular materials. The amount of bound rubber is given by the following equations:[89]

$$B = 1 - \int_0^\infty w(y)\exp(-qy)dy, \quad q = cPM_0 / A_0N_A = cPM_0D / N_A,$$
$$y = M / M_0 \qquad [7.23]$$

where:

w(y)dy	molar mass distribution
q	fraction of adsorbed segments
y	number of segments per polymer chain (degree of polymerization)
c	filler loading (filler to polymer mass ratio)
P	specific surface area of filler
M_0	molar mass of segment
M	molar mass of polymer
A_0	filler surface area per one active site
N_A	Avogadro number

D number of active sites per unit filler surface area

Eq 7.23 can be converted to the following form:

$$B = \gamma \frac{4+\gamma}{(2+\gamma)^2}, \quad \gamma = cP\overline{M}_w D / N_A \qquad [7.24]$$

where:

γ number of adsorbed segments per primary mass average molecule (the so-called adsorption index)
$\overline{M}_w$ mass average molar mass

Specific bound rubber, L, is another factor, frequently used in comparative studies:

$$L = \lim_{cP \to 0} (B / cP) = D\overline{M}_w / N_A \qquad [7.25]$$

It is a very convenient factor because it allows the amount of bound rubber and the available active surface to be related.

In laboratory practice, a small sample of rubber is extracted with solvent (usually toluene) at room temperature for a specified period of time (1 week) and the percentage of bound rubber, R_B, is calculated from the equation:[46]

$$R_B = \frac{W_{fg} - W[m_f / (m_f + m_p)]}{W[m_p / (m_f + m_p)]} \times 100 \qquad [7.26]$$

where:

W_{fg} weight of carbon black and gel
W weight of specimen of rubber taken for extraction
m_f weight of filler in composition
m_p weight of polymer in compound

In order to establish the nature of the bonds, the specimen is also treated with ammonia. Under these conditions only chemically bound rubber remains absorbed on the filler's surface and physically bound polymer is extracted. Silica-rubber gels contain mostly physical bonding.

The temperature of extraction has an effect on the result of the determination (Figure 7.19). At moderate temperatures, there is very little change in the amount of bound rubber determined. At temperatures above 70°C there is substantial increase in the amount of extracted rubber. This data shows that most carbon black is adsorbed by physical forces.

The amount of bound rubber depends on carbon black loading (Figure 7.20).[57] Experimental studies[35,46] show that small additions of carbon black (below 40 phr) obey different relationship than larger additions. The cross-section of both relationships gives a critical coherent loading. This data also shows that bound rubber increases rapidly above 30 phr. Above 80 phr, the bound rubber content begins to level off. NMR studies show a very restricted chain mobility above 80 phr.[57]

Figure 7.21 shows that bound rubber increases as the surface area of carbon black increases.[35,46] This is a classical experiment which shows that the amount of bound rubber depends on the surface area of the filler. High structure carbon blacks

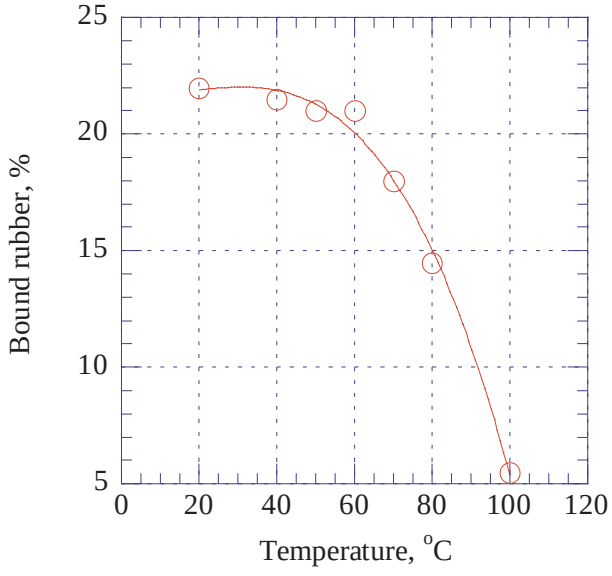

Figure 7.19. Bound rubber as a function of extraction temperature for N330. [Adapted, by permission, from Wolff S, Wang M-J, Tan E-H, *Rubb. Chem. Technol*., **66**, No.2, 1993, 163-77.]

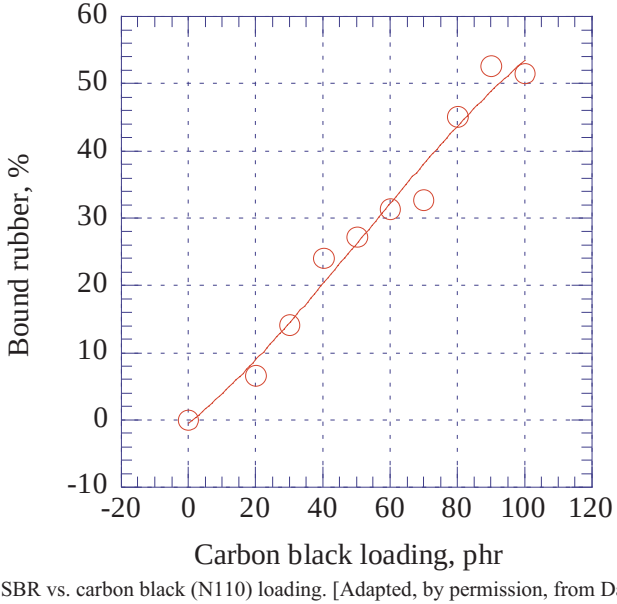

Figure 7.20. Bound SBR vs. carbon black (N110) loading. [Adapted, by permission, from Datta N K, Choudhury N R, Haidar B, Vidal A, Donnet J B, Delmotte L, Chezeau J M, *Polymer*, **35**, No.20, 1994, 4293-9.]

adsorb more rubber than do low structure carbon blacks, having the same surface area, because of the increased probability of multiple adsorption, less graphitization, and a higher tendency to break aggregates during mixing.[89]

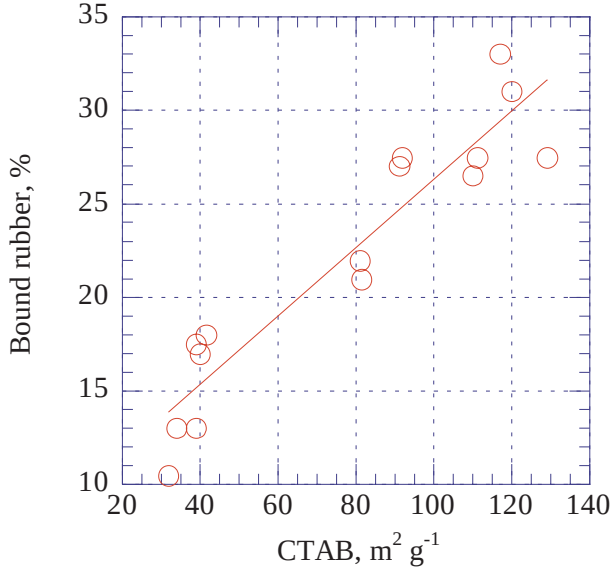

Figure 7.21. Bound rubber vs. CTAB surface area for various carbon blacks at 50 phr loading in SBR. [Adapted, by permission, from Wolff S, Wang M-J, Tan E-H, *Rubb. Chem. Technol*., **66**, No.2, 1993, 163-77.]

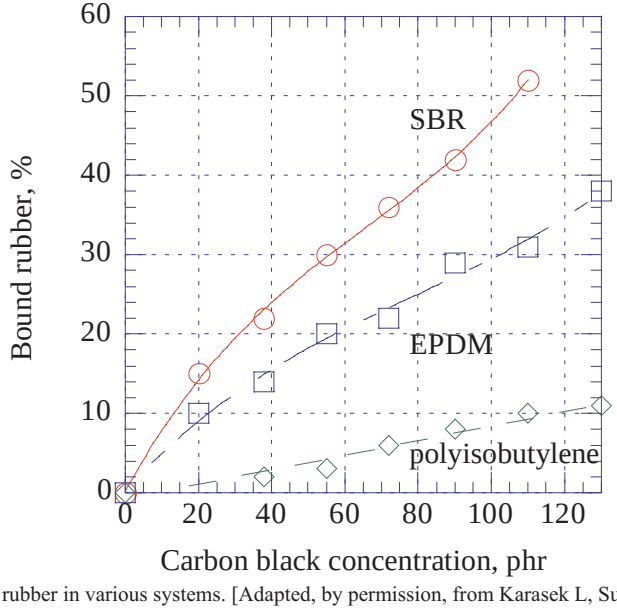

Figure 7.22. Bound rubber in various systems. [Adapted, by permission, from Karasek L, Sumita M, *J. Mat. Sci.*, **31**, No.2, 1996, 281-9.]

The type of rubber also has an influence on the amount of bound rubber (Figure 7.22).[84] It depends on the chemical structure of the rubber, unsaturations, and on the thermal, thermo-mechanical, and oxidative stability of the rubber.

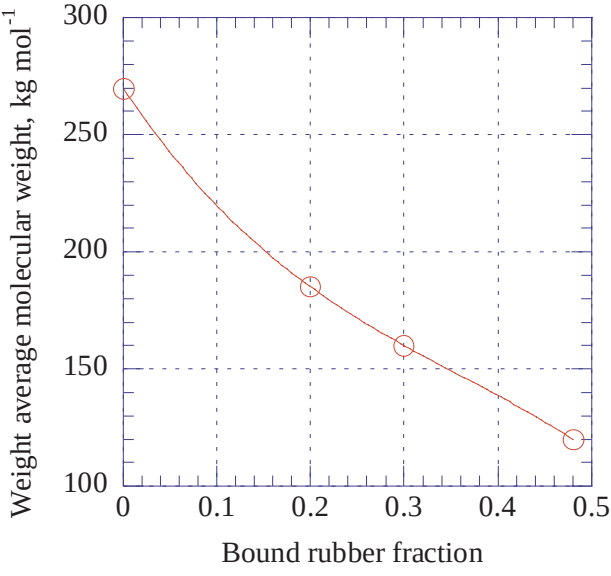

Figure 7.23. Molecular weight of extracted rubber vs. amount of bound rubber. [Adapted, by permission, from Karasek L, Sumita M, *J. Mat. Sci.*, **31**, No.2, 1996, 281-9.]

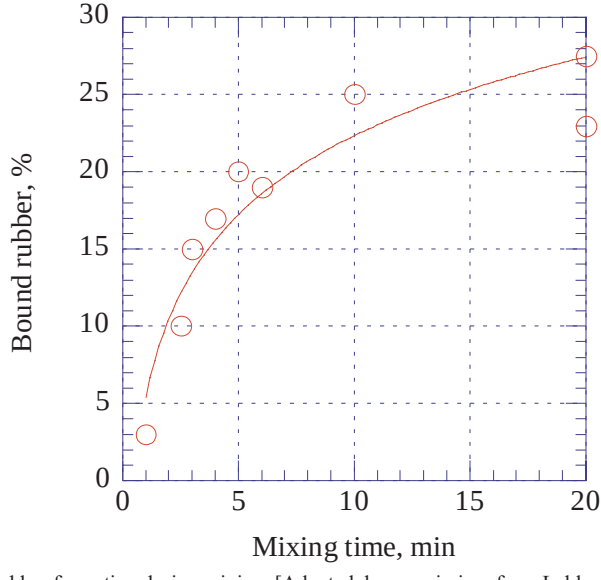

Figure 7.24. Bound rubber formation during mixing. [Adapted, by permission, from Leblanc J L, *Prog. Rubb. Plast. Technol*., **10**, No.2, 1994, 112-29.]

Longer polymer chains are preferentially absorbed by carbon black. Figure 7.23 shows the molecular weight of extracted rubber vs. the amount of bound rubber. Because of the preferential adsorption of longer chains, the molecular weight of extracted rubber decreases as the amount of bound rubber increases.

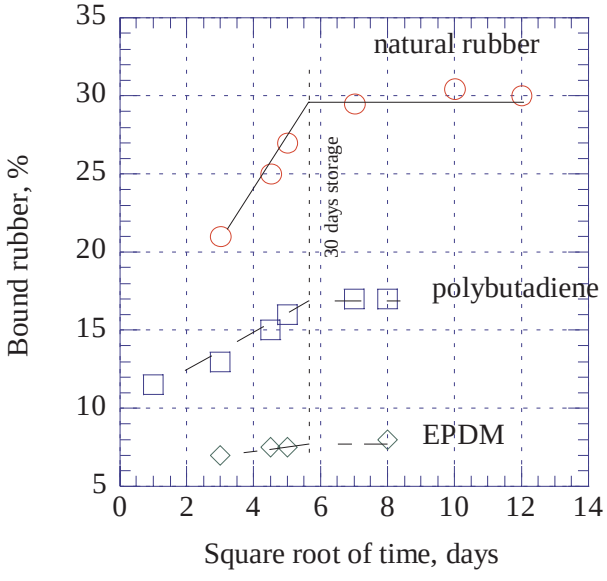

Figure 7.25. Bound rubber vs. storage maturation. [Adapted, by permission, from Leblanc J L, *Prog. Rubb. Plast. Technol*., **10**, No.2, 1994, 112-29.]

Mixing energy, mixing time, and the processing temperature are the parameters affecting the amount of the bound rubber. Figure 7.24 shows the effect of mixing time.[45] There is a certain effective mixing time which is required to attain an equilibrium state. Extended mixing beyond this point causes much smaller changes in bound rubber. There is also a period at the beginning of mixing during which the wetting and the breakdown of aggregates occur. During this induction period, only a small gain in bound rubber was observed.

Not only mixing increases bound rubber but also the storage time. This is called storage maturation (Figure 7.25).[45] This maturation process is very long because it involves a diffusion which is very slow process with macromolecular materials.

Chemical modification of filler surface reduces the surface area available for interaction. This reduces bound rubber (Figure 7.26).[69,93] The quantity of adsorbing additives on the filler surface must be strictly controlled because these additives compete with the reinforcing effect of the bound rubber. Thermal treatment of rubber increased the quantity of bound rubber but only when rubber was added prior to the addition of low molecular processing additives.[94] This shows that there was competition between the low molecular additive and the rubber for adsorption sites.

When the behavior of carbon black and silica is compared in compounded rubber, it is evident that silica adsorbs less rubber than carbon black. In addition to the differences in the chemical compositions of the surfaces this difference is caused by the differences in the dispersive components of surface energies of each filler. Car-

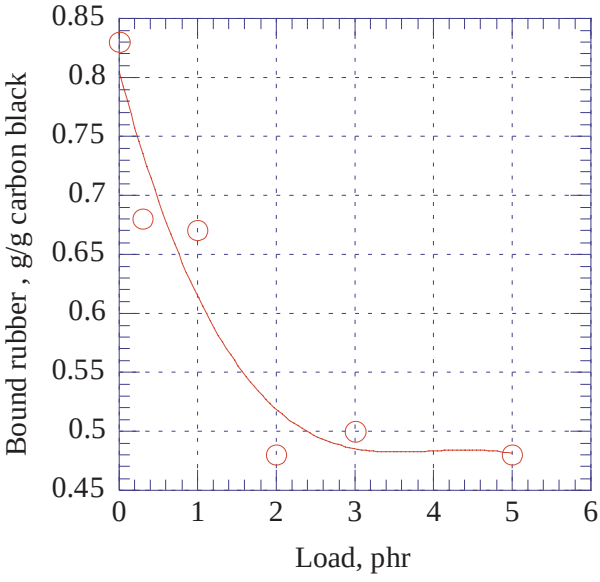

Figure 7.26. Effect of multifunctional additive on bound rubber. [Adapted, by permission, from Ismail H, Freakley P K, Sheng E, *Eur. Polym. J.*, **31**, No.11, 1995, 1049-56.]

bon black has higher dispersive component of surface energy than silica which is the reason for its better dispersion and interaction.[95,96]

The atomic force microscope is used to observe bound rubber on the filler surface.[97] The highest concentration of bound rubber was found in the regions between carbon black particles. A further review of the theory of gel formation can be found in the literature.[98] In the case of some polymers, an uncertainty exists as to whether the determined values are correct because of their solubility (or its lack).[77] Polyethylene is an example. In addition to the complication of solubility, polyethylene modified by maleic anhydride can form covalent bonds with the filler which substantially increases the amount of filler bound polymer.[77] Solvents which interact poorly with silica do not affect the polymer-filler linkages and they give high readings.[99] Also, treatment with ammonia may give a confusing result in the presence of a filler which has been treated previously with low molecular weight substances. Ammonia treatment either removes low molecular substances or reacts with the polymer, which increases the amount of gel formed.[99]

7.13 DEBONDING

Debonding (also called dewetting) is one mechanism of the failure of filler reinforced composites which are subjected to either continuous stress or fluctuating stresses. Debonding may also be used as a method of production for some of the materials discussed in Section 7.3.

Eq 7.15 gives a simple description of the stress acting on an isolated particle. In reality, more particles are involved in the dissipation of local stresses in filled

materials. The interacting stress fields of neighboring particles modify Eq 7.15:[100,101]

$$\sigma^D = \left(-\frac{\sigma^T}{2} + C\sqrt{\frac{W_{mf}}{R}} \right)(1 + m\phi^{1/3}) \qquad [7.27]$$

where:

σ_D	debonding stress
σ_T	thermal stress
C	constant
W_{mf}	reversible work of adhesion
R	radius of inclusion (filler)
m	constant
ϕ	fraction of inclusion (filler)

This equation shows that debonding stress increases with adhesion and filler fraction and decreases with particle size. Figure 7.27 shows the effect of particle size on prediction of yield stress based on the debonding simulated by an equation derived from Eq 7.27. Decreasing particle size increases the stress required for debonding.

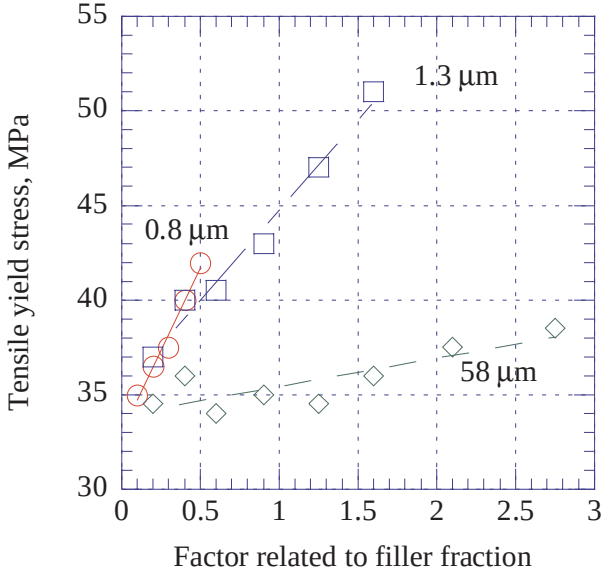

Figure 7.27. Yield stress prediction for different particle sizes. [Adapted, by permission, from Pukanszky B, Voros G, *Polym.Composites*, **17**, No.3, 1996, 384-92.]

Figure 7.28 shows that the tensile strength (reduced to account for the volume fraction of the filler and its interaction) increases with the volume fraction of the filler.[101]

Figure 7.29 shows that coefficient of interaction increases as adhesion increases. Calcium carbonate is treated to increase filler-polymer interaction. Fig-

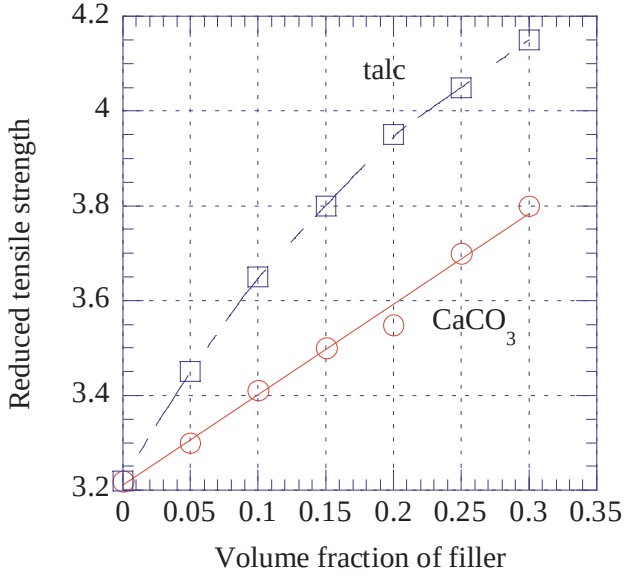

Figure 7.28. Reduced tensile strength vs. volume fraction of filler. [Adapted, by permission, from Pukanszky B, Belina K, Rockenbauer A, Maurer F H J, *Composites*, **25**, No.3, 1994, 205-14.]

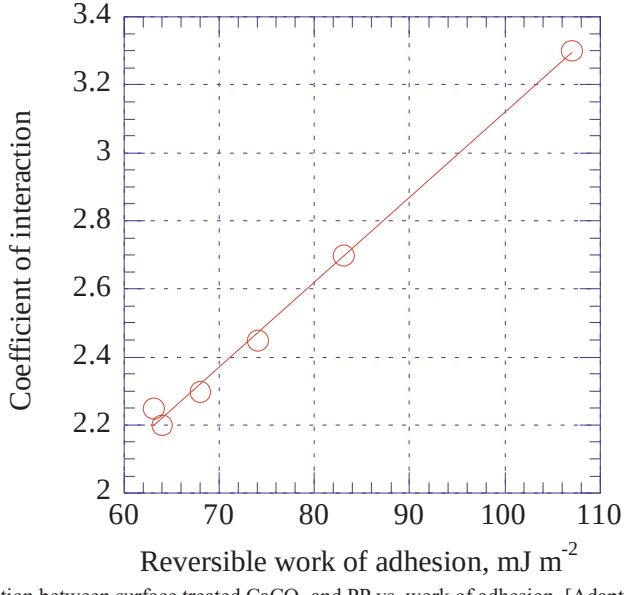

Figure 7.29. Interaction between surface treated $CaCO_3$ and PP vs. work of adhesion. [Adapted, by permission, from Pukanszky B, Belina K, Rockenbauer A, Maurer F H J, *Composites*, **25**, No.3, 1994, 205-14.]

ure 7.29 demonstrates that the effect was achieved. Figures 7.27-7.29 give experimental evidence that Eq 7.27 is generally correct.

The typical stress-strain behavior of filled composites has three stages: elastic, debonding, and crazing or shear yielding. These stages are related to the state of filler-matrix bond.[102-5] Initially all filler particles, having a volume fraction, ϕ, are bonded to the matrix (bonded filler fraction, $\phi_b = \phi$). Under stress, particles gradually debond and new fraction of debonded particles, ϕ_d, is formed ($\phi_b = \phi - \phi_d$). The fraction of completely debonded material is now $\phi_d = \phi$ and $\phi_b = 0$. This has been used in a practical way to obtain a permeable membrane from highly filled material after a stretching process.[31] Two important principles can be derived from this analysis of filler fractions. One is the rate of debonding and the other is the volume increase due to the debonding. The rate of debonding is expressed as

$$\frac{d\phi_d}{dt} = (\phi - \phi_d) K\sigma \exp(B\bar{\sigma}) \qquad [7.28]$$

where:

t	time
K	debonding rate constant
σ	nominal stress
$\bar{\sigma}$	effective stress
B	debonding rate constant

The rate of debonding decreases as the number of debonded particles increases and as the stress increases. The debonding constants characterize the interaction and the influence of neighboring particles. Their values depend on the filler concentration and on the adhesion of the filler to the matrix. The volume increase due to debonding is given by the equation:

$$\varsigma_d = \int_0^\infty \phi_d d\varepsilon \qquad [7.29]$$

where:

ε	strain

The volume increase depends on the filler fraction and on the applied strain. This is confirmed in practice.[31] Debonding correlates with loss of stiffness. The first part of the stress-strain curve (elastic stage) is related to the strains beyond which debonding occurs. In glass bead filled polypropylene, this strain was 0.7%.[106]

In mixtures of particles, the stress of debonding is not uniform. Higher stress is needed to debond from smaller particles.[107] Adhesion is inversely proportional to the cube root of the diameter of the particles.[107] Experiments confirmed that large particle sized filler decreased the tensile strength of composites.[5] The filler concentration effect is not linear. Up to a certain concentration, filler did increase the tensile properties but beyond certain level there is a reverse effect.[108] This may relate to the interactions described in previous sections where the quality of bonding (weak or strong) depended on filler concentration.

A simple equation is derived from the first law of thermodynamics:[109]

$$\delta U = \delta U_{strain} + \delta U_{surface} = \delta W + \delta Q \qquad [7.30]$$

where:

U	energy
W	work
Q	heat

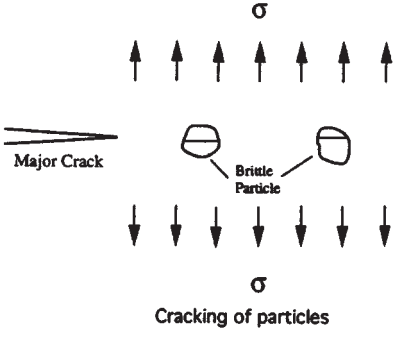

Figure 7.30. Possible crack growth mechanism. [Adapted, by permission, from Xu X X, Crocrombe A D, Smith P A, *Int. J. Fatigue*, **16**, No.7, 1994, 469-77.]

Figure 7.31. Particle splitting. [Adapted, by permission, from Li J X, Silverstein M, Hiltner A, Baer E, *J. Appl. Polym. Sci.*, **52**, No.2, 1994, 255-67.]

This energy balance depends on the energy of the applied strain and the energy of surface. We have consistently assumed that the energy input is lower than the cohesive energy of filler particles. But this is not always true.[110-112]

The mechanical strength of the filler particle may be lower than the adhesive bond strength between the filler and the matrix. This effect is illustrated in Figure 7.30. Concentrated stress causes particle cracking. An SEM micrograph of this event is illustrated in Figure 7.31.

7.14 MECHANISMS OF REINFORCEMENT

Einstein developed the concept of hydrodynamic reinforcement which is expressed by the equation:

$$f = \frac{\eta}{\eta_0} = 1 + 2.5\phi \qquad [7.31]$$

where:

f	hydrodynamic reinforcement factor
η	viscosity of suspension
η_0	viscosity of solvent
ϕ	filler volume fraction

This simple model was later extended by Guth and Gold to include interparticular disturbances. One form of this model is given by Eq 7.6. This model modified by Thomas fits some experimental data:

$$f = 1 + 2.5\phi + 10.05\phi^2 + A\exp(B\phi) \qquad [7.32]$$

where:
A coefficient = 0.00273
B coefficient = 16.6

Figure 7.32 shows that Guth & Gold equation fits data for lower filler volume fractions but Thomas model gives a good prediction of experimental results throughout a very broad range of filler concentrations.[113] This model is fairly universal and it is one of the popular models used for interpretation of experimental data. At the same time, it is clearly visible that the model does not consider most factors, discussed throughout this chapter, which are thought to influence reinforcement of polymers. In one recent review[114] on polymer reinforcement, it is stressed that no consistent model exists (except for the above equations derived from Einstein's concept) which may be used to follow polymer reinforcement. Because of the lack of phenomenological model there are numerous publications which deal with the subject of experimental data by proposing empirical relationships or microscopic models which can explain observed results.[34,35,38,42,59,64,65,115-20] Some findings are discussed below together with much earlier proposal which still remains valid.

One earlier model was developed by Dannenberg to explain observations of behavior of compounded rubber.[121] Figure 7.33 shows how this model works. Polymer chains are connected with filler particles. Depending on strain, chains remain relaxed, are fully extended, slip, or matrix undergoes structural changes. It is im-

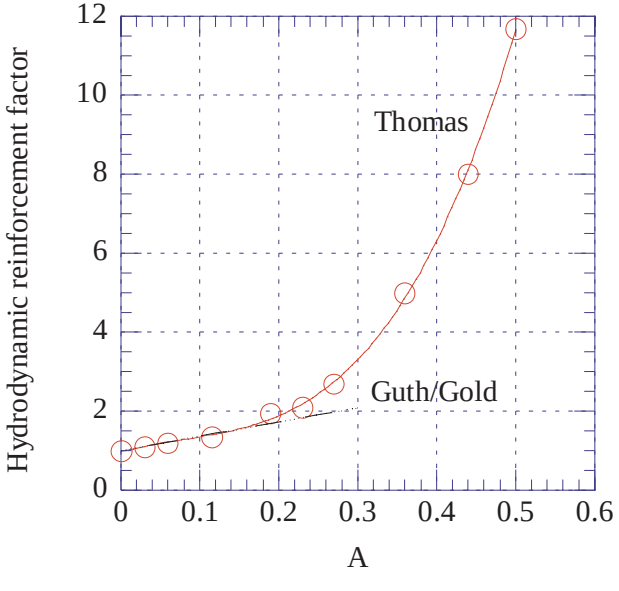

Figure 7.32. Hydrodynamic reinforcement factor vs. filler volume fraction. [Adapted, by permission, from Eggers H, Schummer P, *Rubb. Chem. Technol.*, **69**, No.2, 1996, 253-65.]

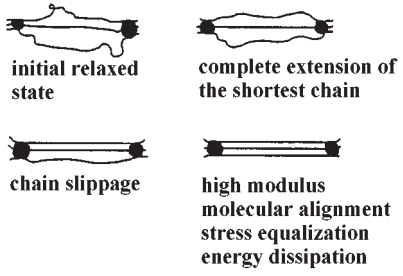

Figure 7.33. Molecular slippage model. [Adapted, by permission, from Dannenberg E M, *Rubber Chem. Technol*., **48**, 1975, 410.]

portant model which explains why certain stress is fully relaxed and larger stresses cause changes in the material but, at the same time it is only descriptive model – not useful in interpretation of experimental data.

Model previously developed by Kraus[122] has got additional interpretation in recent works.[113] Kraus gave simple equation:

$$\phi_{eff} = \beta\phi \qquad [7.33]$$

where:

ϕ_{eff} effective concentration of filler
β effectiveness factor
ϕ filler volume fraction

On surface it is very simple model but effective concentration of filler includes observation that some layer of polymer is bound to the surface of filler and the mechanisms of this bonding is mathematically expressed by effectiveness factor. The recent model assumes that filler particles are spheres which might be connected to form chain-like agglomerates. Each particle is surface coated with matrix polymer. The elastomeric layer is considered immobilized. The effective filler volume is higher than filler volume fraction by the amount of adsorbed polymer. The effectiveness factors is given by equation:

$$\beta = \frac{V_{sphere} + V_{layer} + n\Delta V}{V_{sphere}} = 1 + 6\frac{h}{d_p} + 12\left(1 - \frac{n}{4}\right)\left(\frac{h}{d_p}\right) + 8\left(1 - \frac{n}{2}\right)\left(\frac{h}{d_p}\right) \qquad [7.34]$$

where:

V volume
n mean number of adjacent particles
d_p mean particle diameter

Figure 7.34 shows that the model fits experimental data for carbon black and silica particles.

Several performance characteristics of rubber such as abrasion resistance, pendulum rebound, Mooney viscosity, modulus, Taber die swell, and rheological properties can be modeled by Eq 7.34.[34] A complex mathematical model, called "links-nodes-blobs" was also developed and experimentally tested to express the properties of a filled rubber network system.[42] Blobs are the filler aggregates, nodes are crosslinks and links are interconnecting chains. The model not only allows for

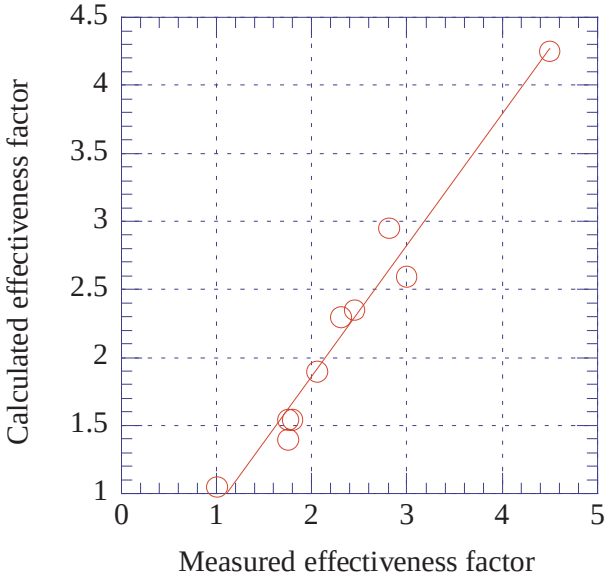

Figure 7.34. Modeling of effectiveness factor. [Adapted, by permission, from Eggers H, Schummer P, *Rubb. Chem. Technol*., **69**, No.2, 1996, 253-65.]

positional changes but assumes the fracture of links. Ten different rubbers were tested and simulated according to the model with good correlation. The success of this percolation model for inelastic filler network indicates that computerized predictions will soon be able to give much closer approximations of experimental results.

Figure 7.15 shows pictorial elements of another model which has been proposed.[38,65] This model was examined by WAXS analysis. An assumption was made that the composite consists of rubber matrix, filler particle, and boundary layer, which diffract waves without interfering with each other. The total radial density difference function, σ_{total}, was calculated from the following equation:

$$\sigma_{total} = (1 - v_F - v_B)\sigma_M + kv_F\sigma_F + cv_B\sigma_B \qquad [7.35]$$

where:

v_F	volume fraction of filler
v_B	volume fraction of boundary layer
σ_M	radial density difference function of rubber matrix
σ_F	radial density difference function of filler particle
σ_B	radial density difference function of boundary layer
k, c	normalization constants due to different scattering power of carbon black and adhesion layer

This model characterizes surface contacts, deals with agglomerates, and explains rubber swelling. It was further developed to characterize reinforcement as a non-Gaussian phenomenon.[38] The model deals with intra-cluster forces and the stress-strain cycle. It is used in the experimental part on uniaxial compression to

explain observed anisotropy of filler-rubber contacts. This is another example of the progress being made in the fundamental treatment of reinforcement.

Rheological tests can also be used to determine the reinforcing potential of silica.[35] The following equation can be used:

$$\frac{D_{max} - D_{min}}{D^0_{max} - D^0_{min}} - 1 = \alpha_F \frac{m_F}{m_P} \qquad [7.36]$$

where:

$D_{max} - D_{min}$	torque difference of filled system
$D^0_{max} - D^0_{min}$	torque difference of the gum
m_F/m_P	filler loading
α_F	filler constant characterizing morphology of filler

Eq 7.36 was used to evaluate the effect of filler type and loading on rebound, modulus, compression. It also permits a comparison with the parameters which characterize morphology.

The distance between aggregates, δ_{aa}, can be obtained from the following equation:[120]

$$\delta_{aa} = \frac{6000}{\rho S}(k\phi^{-1/3}\beta^{-1/3} - 1)\beta^{1.43} \qquad [7.37]$$

where:

ρ	density of filler
S	specific surface area of filler
k	constant based on filler packing
β	expansion factor (or ratio of effective filler volume fraction to filler volume fraction)

The distance between aggregates is a value which correlates with many properties of filled rubber. Figure 7.35 gives an example of the correlation with tanδ.[120] Other applications were made with these properties: ball rebound, effect of graphitization on properties of carbon black and parameters of carbon black which characterize structure.

Some results of experimental studies have been interpreted based on the Anderson-Farris model.[123,124] This model is based on assumptions from a modified first law of thermodynamics:[119]

$$\delta Q + \delta W = \delta U + G_c \delta A \qquad [7.38]$$

where:

δQ	net heat transferred into the system
δW	net external work done on the system
δU	net internal energy in the system
$G_c\delta A$	the surface energy dissipated

This equation is based on a model assuming that the work energy put into the system is either stored as internal strain energy or is used to form a new surface area through debonding. Based on these assumptions, several functional relationships were developed to characterize energy released, uniaxial tensile, change in surface

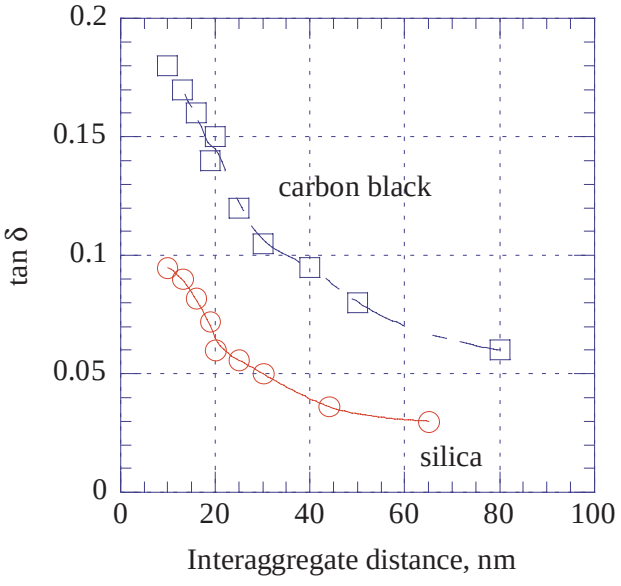

Figure 7.35. tanδ of natural rubber filled with carbon black and silica vs. interaggregate distance, δ_{aa}. [Adapted, by permission, from Wang M-J, Wolff S, Tan E-H, *Rubb. Chem. Technol*., **66**, No.2, 1993, 178-95.]

area, changes in modulus, and Poisson ratio. From relationships, the model can be applied to predict many properties of filled materials. Ten samples of HDPE containing glass beads were used to verify the model.[119] The results show that the model gave a very good prediction of the stress-strain curve. The model predicts nonlinearity due to the particles debonding.

Several other models were proposed based on a series of studies.[115,116,118] These models address specific cases related to work done on experimental materials. A broad discussion of the mechanisms of reinforcement can be found in the specialized monograph by one of the experts in the field.[125] There has been a concerted effort to analyze materials in many different ways and we have tried to present much of this work in this chapter. Many successful attempts have been made to develop universal relationships which explain the reasons for reinforcement and material behavior under external stresses.

7.15 BENEFITS OF ORGANIZATION ON MOLECULAR LEVEL

This section is not intended as a list of all the benefits of interphase formation. They are the subject of this book and the properties of materials are discussed in detail in the individual chapters. It is not appropriate to identify a single property of a material as the most significant. Here are some concluding remarks and examples of other benefits. This will perhaps show that interfacial interactions are not used only for reinforcement.

A recent paper[126] brings several points of interest for this discussion. Examples of two materials (abalone shell and spider web fiber) are examined. These natural materials benefit from the molecular organization to the extent still not conquered by the scientific discoveries. Abalone shell is composed of calcium carbonate and polysaccharides and proteins as binders. The impact resistance of this material is remarkable. Calcium carbonate is not known in our applications as reinforcing material. Natural material differs in structural organization and interaction with the binder from man made materials. Similarly, the strength of fibers produced by spiders is achieved through the morphology of the natural polymer. Again, no man made polymer has been able to duplicate this level of performance. Although these examples show that the current technology has been unable to achieve the remarkable performance of these natural materials, recent developments provide evidence that rapid progress is being made towards better performing materials.

Natural products are highly compatible with other surrounding materials particularly, growing tissues. In the future, materials used for medical applications may have the ability to influence one's body to deposit layers of material which is compatible with the body. By crystallization of filler-like materials in the presence of body fluids, surfaces have been artificially synthesized to be similar to natural materials. It may be possible to induce grafting of a surface through the natural processes occurring in the organism. A goal of such work would be to develop highly specific interfaces which will be recognized by many organisms and ultimately would be specifically compatible with one.

The third essential point of the cited publication[126] also makes us realize that nature uses a very small number of compounds as building blocks (as demonstrated by the widespread presence of silica or calcium carbonate). But the natural design of these structures builds products of very diverse properties. The design differences are generally not chemical but structural. The important lesson for designers is that it is not the number of available monomers but their sequence and structural organization which imparts their unique properties.

Figure 7.36 shows that natural graphite from Siberia can be used to synthesize copolymers with different properties.[127] An increase in the specific surface area results in the formation of copolymers with shorter blocks. By varying the structure of the filler and its concentration, one is able to tailor copolymers to a desired structure.

The amount of carbon black, its particle size and structure, the filler-matrix interaction, and the processing technique determine the electrical properties of a product. At a certain concentration of filler, the conductivity of the material increases dramatically. This concentration is known as the percolation threshold and the conductivity of the material is expressed by equation:

$$\sigma = \sigma_0 (X - X_c)^s \qquad [7.39]$$

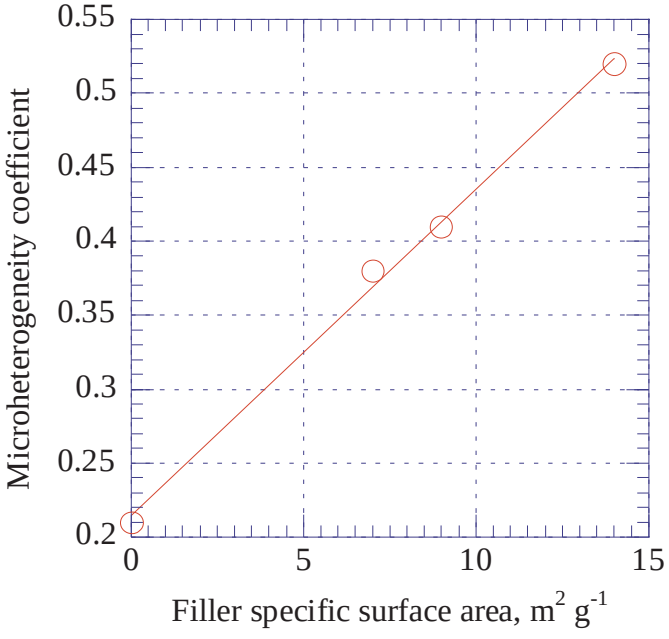

Figure 7.36. Influence of filler's surface on microheterogeneity coefficient of copolymers. [Adapted, by permission, from Vasnev V A, Tarasov A I, Istratov V N, Ignatov V N, Krasnov A P, Kuznetsov A I, Surkova I N, *Reactive & Functional Polym.*, **26**, Nos.1-3, 1995, 177-83.]

where:

σ_0	conductivity of filler particles
X	volume fraction of filler
X_c	volume fraction of filler at percolation threshold
s	a quantity determining the power of the conductivity increasing above X_c

Figure 7.37 shows the effect of the percolation threshold on a material's conductivity.[128] In this example the material has s = 7.75 which is a very high value compared with other data found in the literature. The value of s depends on the structure and surface area of the filler used for production of the material. The filler properties determine the interface formation which permit the electron tunneling mechanism to occur.

Figure 3.38 shows that reaction between $Al(OH)_3$ and dicarboxylic acid anhydride affects the sedimentation volume of filler.[129] The limiting value of sedimentation was obtained by modifying the filler surface with a monolayer of a suitable modifier. A similar modification affects the performance of this filler in polymer-filler composites. Thus, different properties were affected by the surface coverage of filler and by the filler-matrix interactions.

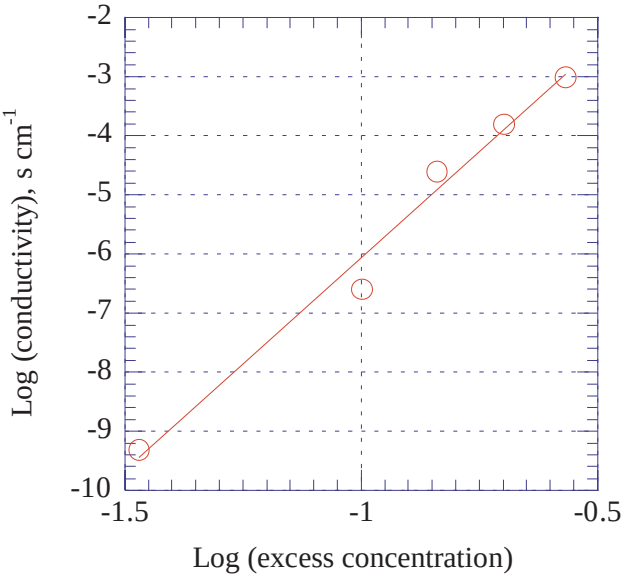

Figure 7.37. Conductivity of SBR-carbon black vs. excess concentration. [Adapted, by permission, from Karasek L, Meissner B, Asai S, Sumita M, *Polym. J. (Jap.)*, **28**, No.2, 1996, 121-6.]

REFERENCES

1 Shuhong Wang, Mark J E, *Macromol. Reports*, **A31**, Nos.3 & 4, 1994, 253-6.
2 Chen L, Liu K, Yang C Z, *Polym. Bull.*, **37**, No.3, 1996, 377-83.
3 Pu Z, Mark J E, Jethmalani J M, Ford W T, *Polym. Bull.*, **37**, No.4, 1996, 545-51.
4 Rosenov M W K, Bell J A E, Antec '97. Conference proceedings, Toronto, April 1997, 1492-8.
5 Kovacevic V, Lucic S, Hace D, Cerovecki Z, *J. Adhesion Sci. Technol.*, **10**, No.12, 1996, 1273-85.
6 Bormashenko E Y, Zagoskin A M, *Int. Polym. Sci. Technol.*, **23**, No.1, 1996, T/80-1.
7 Kano Y, Akiyama S, Yui H, Kasemura T, *Polym. Networks Blends*, **7**, 117-20 (1997).
8 Tchoudakov R, Breuer O, Narkis M, Siegmann A, *Polym. Networks Blends*, **6**, 1-8 (1996).
9 de Candia F, Carotenuto M, Gargani L, Guadagno L, Lauretti E, Renzulli A, *Kaut. u. Gummi Kunst.*, **49**, No.2, 1996, 99-101.
10 Guerbe L, Freakley P K, *Kaut. u. Gummi Kunst.*, **48**, No.4, 1995, 260-9.
11 Papathanasiou T D, *Int. Polym. Processing*, **11**, No.3, Sept.1996, 275-83.
12 Ogadhoh S O, Papathanasiou T D, *Composites Part A: Applied Science and Manufacturing*, **27A**, No.1, 1996, 57-63.
13 Chang Ho Suh, White J L, *Polym. Engng. Sci.*, **36**, No.11, 1996, 1521-30.
14 Klapcinski T, Galeski A, Kryszewski M, *J. Appl. Polym. Sci.*, **58**, No.6, 1995, 1007-13.
15 Wagner A H, Kalyon D M, Yazici R, Fiske T J, Antec '97. Conference proceedings, Toronto, April 1997, 996-1000.
16 Kim K J, White J L, *J. of Non-Newtonian Fluid Mechanics*, **66**, Nos.2/3, 1996, 257-70.
17 Fiske T, Gokturk H S, Yazici R, Kalyon D M, Antec '97. Conference proceedings, Toronto, April 1997, 1482-6.
18 Dreibelbis G L, Antec 95. Volume III. Conference proceedings, Boston, Ma., 7th-11th May 1995, 4374-6.
19 Allan P S, Bevis M J, *Materials World*, **2**, No.1, 1994, 7-9.
20 Barbosa S E, Kenny J M, Ercoli D R, Bibbo M A, Antec '97. Conference proceedings, Toronto, April 1997, 2189-93.
21 Lee S C, Yang D Y, Youn J R, Antec '97. Conference proceedings, Toronto, April 1997, 642-8.
22 Gerard P, Raine J, Pabiot J, Antec '97. Conference proceedings, Toronto, April 1997, 526-31.
23 Suh C H, White J L, Antec '96. Vol.I. Conference Proceedings, Indianapolis, 5th--10th May 1996,

p.958-62.
24 Wagner A H, Kalyon D M, Tan V, Antec '96. Volume II. Conference proceedings, Indianapolis, 5th-10th May 1996, 2195-9.
25 Barbosa S E, Kenny J M, Antec '97. Conference proceedings, Toronto, April 1997, 1855-9.
26 Suh C H, White J L, *Polym. Engng. Sci*., **36**, No.17, 1996 2188-97.
27 Rabello M S, White J R, *Polym. Composites*, **17**, No.5, 1996, 691-704.
28 Wada N, Uchiyama Y, Hosokawa M, *Int. Polym. Sci. Technol*., **21**, No.3, 1994, T/53-63.
29 Wu Y, Shivpuri R, Lee L J, Antec '97. Conference proceedings, Toronto, April 1997, 1849-54.
30 Merwin L H, Nissan R A, Stephens T S, Wallner A S, *J. Appl. Polym. Sci.*, **62**, No.2, 1996, 341-8.
31 Nakamura S, Kaneko S, Mizutani Y, *J. Appl. Polym. Sci.*, **49**, No.1, 1993, 143-50.
32 Mitsui S, Kihara H, Yoshimi S, Okamoto Y, *Polym. Engng. Sci*., **36**, No.17, 1996, 2241-6.
33 Bagheri R, Pearson R A, *Polymer*, **36**, No.25, 1995, 4883-5.
34 Patel A C, *Kaut. u. Gummi Kunst*., **47**, No.8, 1994, 556-70.
35 Wolff S, *Rubb.Chem.Technol*., **69**, No.3, 1996, 325-46.
36 Li Q, Manas-Zloczower I, Feke D L, *Rubb. Chem. Technol*., **69**, No.1, 1996, 8-14.
37 Tsukuda R, Sumimoto S, Ozawa T, *J. Appl. Polym. Sci*., **59**, No.6, 1996, 1043-6.
38 Kilian H G, Strauss M, Hamm W, *Rubb. Chem. Technol.,* **67**, No.1, 1994, 1-16.
39 Tsagaropoulos G, Eisenberg A, *Macromolecules*, **28**, No.18, 1995, 6067-77.
40 Mandal U K, Tripathy D K, De S K, *Plast. Rubb. Comp. Process. Appln*., **24**, No.1, 1995, 19-25.
41 Bomal Y, Godard P, *Polym. Engng. Sci*., **36**, No.2, 1996, 237-43.
42 Lin C R, Lee Y D, *Macromol. Theory & Simulations*, **5**, No.6, 1996, 1075-104.
43 Wu J, Lerner M M, *Chem. of Mat.*, **5**, No.6, 1993, 835-8.
44 Tsagaropoulos G, Eisenberg A, *Macromolecules*, **28**, No.1, 1995, 396-8.
45 Leblanc J L, *Prog. Rubb. Plast. Technol*., **10**, No.2, 1994, 112-29.
46 Wolff S, Wang M-J, Tan E-H, *Rubb. Chem. Technol*., **66**, No.2, 1993, 163-77.
47 Reis M J, Do Rego A M B, Da Silva J D L, *J. Mat. Sci*., **30**, No.1, 1995, 118-26.
48 Datta S, De S K, Kontos E G, Wefer J M, Wagner P, Vidal A, *Polymer*, **37**, No.15, 1996, 3431-5.
49 Bandyopadhyay S, De P P, Tripathy D K, De S K, *Kaut. u. Gummi Kunst*., **49**, No.2, 1996, 115-9.
50 Ayala J A, Hess W M, Joyce G A, Kistler F D, *Rubb. Chem. Technol*., **66**, 1993, 772.
51 Bandyopadhyay S, De P P, Tripathy D K, De S K, *J. Appl. Polym. Sci*., **61**, No.10, 1996, 1813-20.
52 Datta S, Bhattacharya A K, De S K, Kontos E G, Wefer J M, *Polymer*, **37**, No.12, 1996, 2581-5.
53 Kurian T, De P P, Khastgir D, Tripathy D K, De S K, Peiffer D G, *Polymer*, **36**, No.20, 1995, 3875-84.
54 Sain M M, Kokta B V, Antec '93. Conference Proceedings, New Orleans, La., 9th-13th May 1993, Vol. I, 320-4.
55 Tang L-G, Kardos J L, *Polym. Composites*, **18**, No.1, 1997, 100-13.
56 Yoshinaga K, Nakanishi K, Hidaka Y, Karakawa H, *Composite Interfaces*, **3**, No.3, 1995, 231-41.
57 Tsutsumi K, Ban K, Shibata K, Okazaki S, Kogoma M, *J. Adhesion*, **57**, 1996, 45-53.
58 Hartley P A, Parfitt G P, Pollack L B, *Powder Technol*., **42**, 1985, 35.
59 Kurian T, Khatgir D, De P P, Tripathy D K, De S K, Peiffer D G, *Polymer*, **37**, No.25, 1996, 5597-605.
60 Herzog E, Caseri W, Suter U W, *Coll. Polym. Sci*., **272**, No.8, 1994, 986-90.
61 Cochrane H, Lin C S, *Rubb. Chem. Technol*., **66**, No.1, 1993, 48-60.
62 Gorl U, Rausch R, Esch H, Kuhlmann R, *Int. Polym. Sci. Technol*., **23**, No.7, 1996, T/81-7.
63 Donnet J B, *Kaut. u. Gummi Kunst*., **47**, No.9, 1994, 628-32.
64 Donnet J B, Wang T K, *Prog. Rubb. Plast. Technol*., **11**, No.4, 1995, 261-7.
65 Strauss M, Pieper T, Peng W, Kilian H G, *Makromol. Chem., Macromol. Symp*., **76**, 1993, 131-6.
66 Roche A A, Dole P, Bouzziri M, *J. Adhesion Sci. Technol*., **8**, No.6, 1994, 587-609.
67 El-Shall M S, Slack W, *Macromolecules,* **28**, No.24, 1995, 8456-8.
68 Herd C R, Bomo F, *Kaut. u. Gummi Kunst*., **48**, No.9, 1995, 588-99.
69 Ismail H, Freakley P K, Sheng E, *Eur. Polym. J*., **31**, No.11, 1995, 1049-56.
70 Hedgus C R, Kamel I L, *J. Coatings Technol.*, **65**, No.821, June 1993, 49-61.
71 Mi Y, Chen X, Guo Q, *J. Appl. Polym. Sci*., **64**, 1997, 1267-73.
72 Dufresne A, Lacabanne C, *Polymer*, **34**, No. 15, 1993, 3173-8.
73 Wool R P, Long J M, *Macromolecules*, **26**, No.19, 1993, 5227-39.
74 Gerard J F, Chabert B, *Macromol. Symp*., **108**, 1996, 137-46.
75 Carre A, *J. Adhesion*, **54**, Nos.1-4, 1995, 167-74.
76 Heinrich G, Vilgis T A, *Rubb. Chem. Technol*., **68**, No.1, 1995, 26-36.
77 Hindryckx F, Dubois P, Patin M, Jerome R, Teyssie P, Garcia Marti M, *J. Appl. Polym. Sci.*, **56**, No.9, 1995, 1093-105.

78 Ou Y, Yu Z, Zhu J, Li G, Zhu S, *Chinese J. Polym. Sci.*, **14**, No.2, 1996, 172-82.
79 Pak S H, Caze C, *J. Appl. Polym. Sci*., **65**, 1997, 143-53.
80 Suetsugu K, Sakairi T, *Kobunshi Ronbunshu*, **44**, 1987, 369.
81 Ziegel K D, J. *Colloid Interface Sci.*, **29**, 1969, 72.
82 Shenoy A V, Saini D R, *Polym. Compos*., **7**, 1986, 96.
83 Ou Y C, Yu Z Z, Vidal A, Donnet J B, *J. Appl. Polym. Sci*., **59**, No.8, 1996, 1321-8.
84 Karasek L, Sumita M, *J. Mat. Sci.*, **31**, No.2, 1996, 281-9.
85 Garvey M J, Tadros T F, Vincent B, *J. Colloid Inter. Sci.*, **49**, 1974, 57.
86 Pliskin I, Tokita N, *J. Appl. Polym. Sci*., **16**, 1972, 473.
87 Boluk M Y, Schreiber H P, *Polym. Compos*., **7**, 1986, 295.
88 Maier P G, Goeritz D, *Kaut. u. Gummi Kunst*., **49**, No.1, 1996, 18-21.
89 Meissner B, *Rubb. Chem. Technol*., **68**, No.2, 1995, 297-310.
90 Cohen Addad J P, Euradh '94. Conference Proceedings, Mulhouse, 12th-15th Sept.1994, 25-30.
91 Mark J E, *Macromol. Symp*., **101**, 1996, 423-33.
92 Twiss D F, *J. Chem. Soc*., **44**, 1925, 1067.
93 Ismail H, Freakley P K, Sutherland I, Sheng E, *Eur. Polym. J*., **31**, No.11, 1995, 1109-17.
94 Donnet J B, Wang W, Vidal A, Wang M J, *Kaut. u. Gummi Kunst*., **4**6, No.11, Nov.1993, 866-71.
95 Karasek L, *Int. Polym. Sci. Technol*., **21**, No.10, 1994, T/35-40.
96 Wolff S, Wang M J, Tan E H, *Kaut. u. Gummi Kunst*., **47**, No.12, 1994, 873-84.
97 Niedermeier W, Raab H, Maier P, Kreitmeier S, Goeritz D, *Kaut. u. Gummi Kunst*., **48**, No.9, 1995, 611-6.
98 Karasek L, Meissner B, *J. Appl. Polym. Sci*., **52**, No.13, 1994, 1925-31.
99 Roychoudhury A, De P P, Roychoudhury N, Vidal A, *Rubb. Chem. Technol*., **68**, No.5, 1995, 815-23.
100 Pukanszky B, Voros G, *Polym.Composites*, **17**, No.3, 1996, 384-92.
101 Pukanszky B, Belina K, Rockenbauer A, Maurer F H J, *Composites*, **25**, No.3, 1994, 205-14.
102 Meddad A, Fisa B, *J. Mater. Sci*., **32**, 1997, 1177-85.
103 Meddad A, Fisa B, *J. Appl. Polym. Sci*., **65**, 1997, 2013-24.
104 Meddad A, Fellahi S, Pinard M, Fisa B, Antec '94. Conference Proceedings, San Francisco, Ca., 1st-5th May 1994, Vol. II, 2284-8.
105 Meddad A, Fisa B, *Macromol. Symp.*, **108**, 1996, 173-82.
106 Sjogren B A, Berglund L A, *Polym. Composites*, **18**, No.1, 1997, 1-8.
107 Babich V F, Lipatov Yu S, Todosijchuk T T, *J. Adhesion*, **55**, Nos.3-4, 1996, 317-27.
108 Dubnikova I L, Gorokhova E V, Gorenberg A Y, Topolkaraev V A, *Polym. Sci., Ser. A*, **3**7, No.9, 1995, 951-8.
109 Vratsanos L A, Farris R J, *Polym. Engng. Sci*., **33**, No.22, 1993, 1458-65.
110 Xu X X, Crocrombe A D, Smith P A, *Int. J. Fatigue*, **16**, No.7, 1994, 469-77.
111 Xu X X, Crocombe A D, Smith P A, *Int. J. Fatigue*, **17**, No.4, 1995, 279-86.
112 Li J X, Silverstein M, Hiltner A, Baer E, *J. Appl. Polym. Sci.*, **52**, No.2, 1994, 255-67.
113 Eggers H, Schummer P, *Rubb. Chem. Technol*., **69**, No.2, 1996, 253-65.
114 Vilgis T A, Heinrich G, *Macromolecules*, **27**, No.26, 1994, 7846-54.
115 Jancar J, *Macromol. Symp*., **108**, 1996, 163-72.
116 Wang Z, *J. Appl. Polym. Sci*., **60**, No.12, 1996, 2239-43.
117 Alpern V, Shutov F, *Prog. Rubb. Plast. Technol*., **11**, No.4, 1995, 268-83.
118 Mele P, Alberola N D, *Composites Sci. & Technol*., **56**, No.7, 1996, 849-53.
119 Wong F C, Ait-Kadi A, *J. Appl. Polym. Sci*., **55**, No.2, 1995, 263-78.
120 Wang M-J, Wolff S, Tan E-H, *Rubb. Chem. Technol*., **66**, No.2, 1993, 178-95.
121 Dannenberg E M, *Rubber Chem. Technol*., **48**, 1975, 410.
122 Kraus G, *Rubber Chem. Technol.*, **44**, 1971, 199.
123 Anderson L L, Farris R J, *Polym. Eng. Sci.*, **28**, 1988, 522.
124 Anderson L L, PhD Thesis. University of Massachussetts, 1989.
125 Lipatov Y S, **Polymer Reinforcement**, *ChemTec Publishing*, Toronto, 1995.
126 Carraher C E, *Polym. News*, **19**, No.2, 1994, 50-2.
127 Vasnev V A, Tarasov A I, Istratov V N, Ignatov V N, Krasnov A P, Kuznetsov A I, Surkova I N, *Reactive & Functional Polym.*, **26**, Nos.1-3, 1995, 177-83.
128 Karasek L, Meissner B, Asai S, Sumita M, *Polym. J. (Jap.)*, **28**, No.2, 1996, 121-6.
129 Liauw C M, Hurst S J, Lees G C, Rothon R N, Dobson D C, *Prog. Rubb. Plast. Technol*., **11**, No.2, 1995, 137-53.